FULL-LENGTH, FIBEROPTIC ESOPHAGEAL PRESSURE MONITOR

Phase I SBIR Grant 1-R43-DK42404-01

Final Report

12 March, 1991

Stefan Begej

This work was performed by Begej Corporation, 5 Claret Ash Road, Littleton, CO, 80127, under Phase I Small Business Innovation Research grant 1-R43-DK42404-01 funded by the National Institute of Diabetes and Digestive and Kidney Diseases, U.S. Department of Health and Human Services, Bethesda, MD, 20892.

FULL-LENGTH, FIBEROPTIC PRESSURE MONITOR

PROJECT SUMMARY

The objective of this program was to explore the feasibility of developing a flexible, full-length, fiberoptic pressure sensor and pressure monitor system suitable for characterizing the motility of the esophagus and associated sphincters.

This objective was partially achieved by the development of a 275 mm long by 8.5 mm diameter optical pressure sensor containing 189 discrete sensor sites distributed in two distinct patterns: the proximal section contained a 250 mm long linear array with 101 sites for measuring the motility of the esophagus, and the distal portion contained a 25 mm long cylindrical array with 88 sites for characterizing sphincter pressures. In addition to the hardware associated with the sensor, an extensive software package was also developed for pressure data acquisition, calibration, processing, and display. It was demonstrated (using synthetic esophageal signals) that the sensor and software could be combined into an effective pressure monitoring system capable of processing voluminous quantity of pressure data and displaying the results in a complete and intuitively-interpretable format.

However, the developed sensor was rigid rather than flexible, as a suitable flexible but highly transparent waveguide material could not be discovered during the course of this program. As a consequence, the sensor was found to be insufficiently sensitive to the pressure range required for the intended medical application (i.e., 0 to 200 mmHg).

It was concluded that development of a full-length flexible esophageal pressure sensor and monitor system is technically feasible, but that additional work would be required regarding the discovery of better flexible and highly-transparent waveguide materials and more sensitive pressure transduction materials.

RIGHTS NOTICE

SBIR RIGHTS NOTICE (APR 1985)

This SBIR data is furnished with SBIR rights under NIDDK grant 1-R43-DK42404-01. For a period of two years after acceptance of all items to be delivered under this contract the Government agrees to use this data for Government purposes only, and it shall not be disclosed outside the Government during such period without permission of the Contractor, except that, subject to the foregoing use and disclosure prohibitions, such data may be disclosed for use by support contractors. After the aforesaid two-year period the Government has a royalty-free license to use, and to authorize others use on its behalf, this data for Government purposes, but is relieved of all disclosure prohibitions and assumes no liability for unauthorized use of this data by third parties. This Notice shall be affixed to any reproductions of this data, in whole or in part.

TABLE OF CONTENTS

1. TECHNICAL AIMS OF THE PROJECT

The overall goal of this project was to develop a innovative, full-length, fiberoptic esophageal pressure monitoring instrument. This device would contribute to improved health-care by offering significantly enhanced performance and lower cost over current methods of characterizing pathological behavior of the esophagus and related organs. The immediate goals of the Phase I project would be to demonstrate the feasibility of modifying an existing fiberoptic pressure sensor technology for this new medical application, and to demonstrate a multi-channel laboratory prototype of a pressure measurement system capable of monitoring the full length of the esophagus. The potential of this research for commercialization is considered to be high, as it directly addresses the needs of gastrointestinal specialists, hospitals, and medical research centers for a versatile, convenient, and low-cost system for manometric characterization of the esophagus. A diagram of the sensor and monitor system as originally proposed are shown in Figure 1, and the principal innovative features listed below:

1. The flexible pressure sensor would contain several hundred pressure sensor sites spaced 2.5 mm apart and extend the full length of the esophageal tract, thereby permitting a <u>complete</u> manometric characterization to be performed on the pharyngoesophageal sphincter, esophagus, and gastroesophageal sphincter with only one or two swallow-actions by the patient. This new sensor would be a marked improvement over conventional devices, as laborious and uncomfortable sensor translation would not be required to characterize the esophageal system. Furthermore, the present problem of sensor dislocation would be avoided, as each swallow action would automatically capture two natural position calibration points consisting of the pharynx and lower esophageal sphincter.

2. The distal portion of the sensor would consist of a 25 mm long cylindrical section containing a circumferential distribution of pressure sensing sites (11 layer x 8 sensor sites per layer). This sensing region would permit characterization of vector pressures associated with non-uniformly contractile organs such as the pharyngoesophageal sphincter.

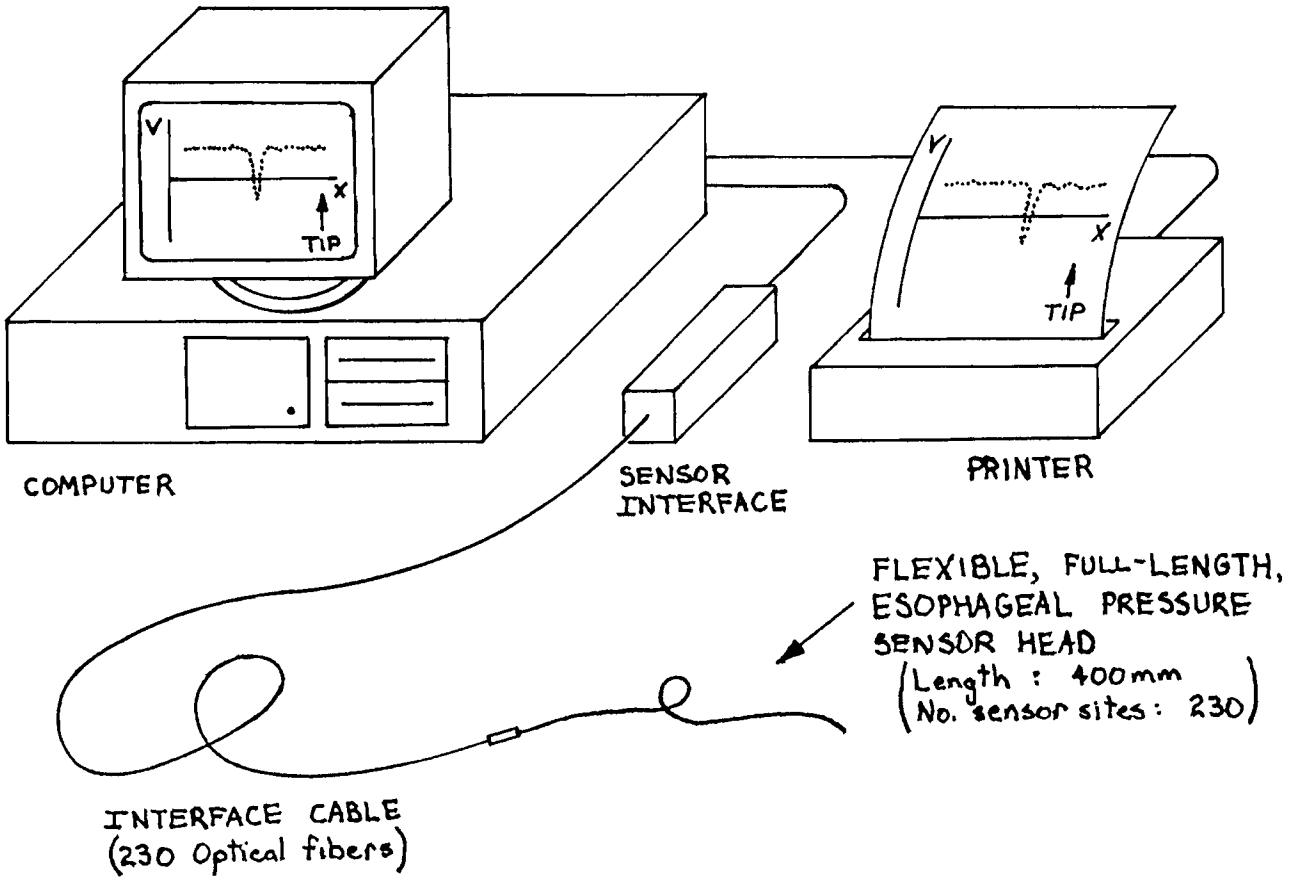

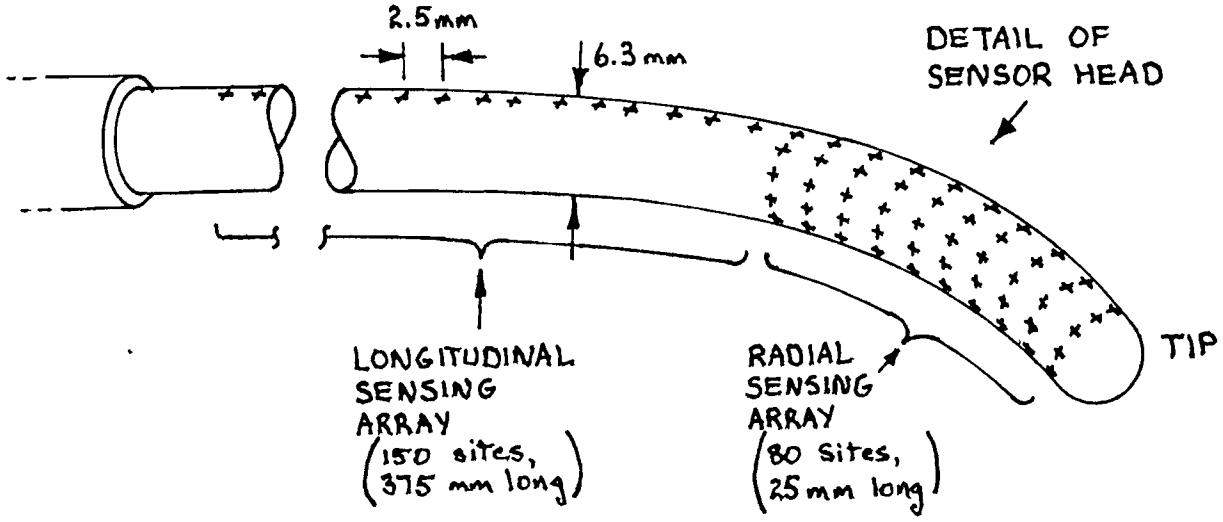

FIGURE 1: Appearance of the originally proposed full-length, fiberoptic esophageal pressure monitor system. The instrument would be capable of collecting several hundred pressure samples along the entire length and in multiple directions about the cylindrical sensor at the distal tip, and to display the data in a processed, intuitively-interpretable format.

3. A computer would be used to create a user-friendly interface for the physician/user, and provide direct and rapid visualization of the entire peristaltic wave and sphincter pressures. For example, the data generated by one swallow event would be automatically processed, and results such as the maximum pressures or peristaltic wave velocity presented in a convenient and intuitively-interpretable graphical format.

4. Unlike presently-used manometric tubes, the optical pressure sensor would be completely sealed, thereby significantly simplifying procedures required for sterilization and re-use.

2. RESEARCH CONDUCTED

This section is divided into four major subsections that will discuss development of the sensor hardware (2.1) and data processing/display software (2.2), evaluation of the sensor system performance (2.3), and conclusions regarding technical feasibility and directions for future work (2.4).

2.1. Sensor Hardware Development

2.1.1. Sensor Development Background

The pressure sensing technology explored in this program utilized the principle of frustrated total internal reflection (FTIR) at an optical surface (Begej [1984]), and is illustrated in Figure 2. Light is injected into the edge of a planar waveguide where it is initially confined by total internal reflection between the parallel faces. A white, textured plastic membrane is placed in contact with one face of the waveguide. Then, pressures exerted against this membrane cause TIR to be frustrated at the contact locations due to light absorbtion by the membrane material. That fraction of the diffuse light emanating from these contact locations that no longer satisfies the angular conditions for TIR within the waveguide is then observed when it exits through the opposite face.

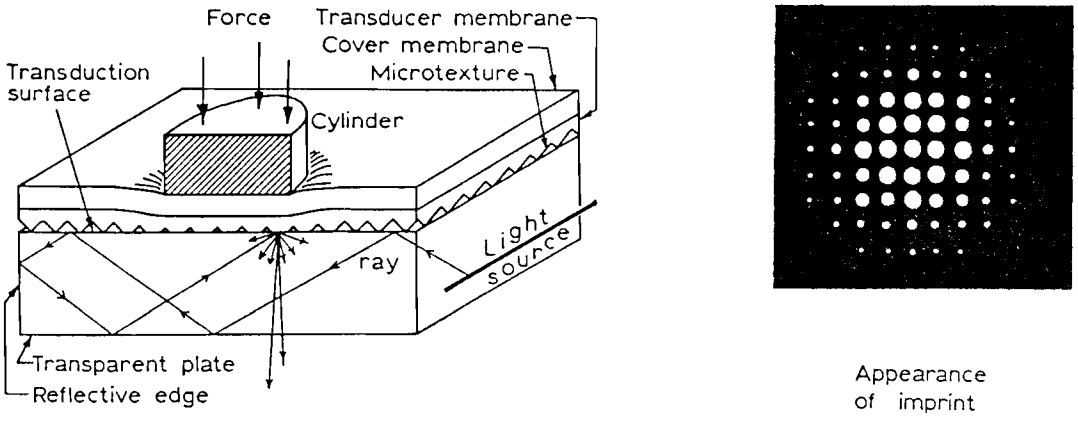

FIGURE 2: General arrangement of components for sensing contact pressure distributions by frustration of total internal reflection (FTIR) at the surface of a waveguide. Diagram at right illustrates how areas subject to higher pressures appear as regions of greater light intensity. From Begej [1984].

Several compact fiberoptic tactile sensors utilizing this sensing technology have been developed by the author for robotic applications. Figure 3 shows an early device (Begej [1985]) which featured a 32 x 32 array of pressure sensor sites, each site being spaced 1 mm apart. This device was interfaced to a computer which performed data acquisition and display functions. Figure 4 shows a more advanced fingertip-shaped tactile sensor subsequently developed for use with a dexterous robotic hand (Begej [1986, 1988a, 1988b]). It featured 256 pressure sensing sites distributed in two surface densities (100/cm^2 and 10/cm^2).

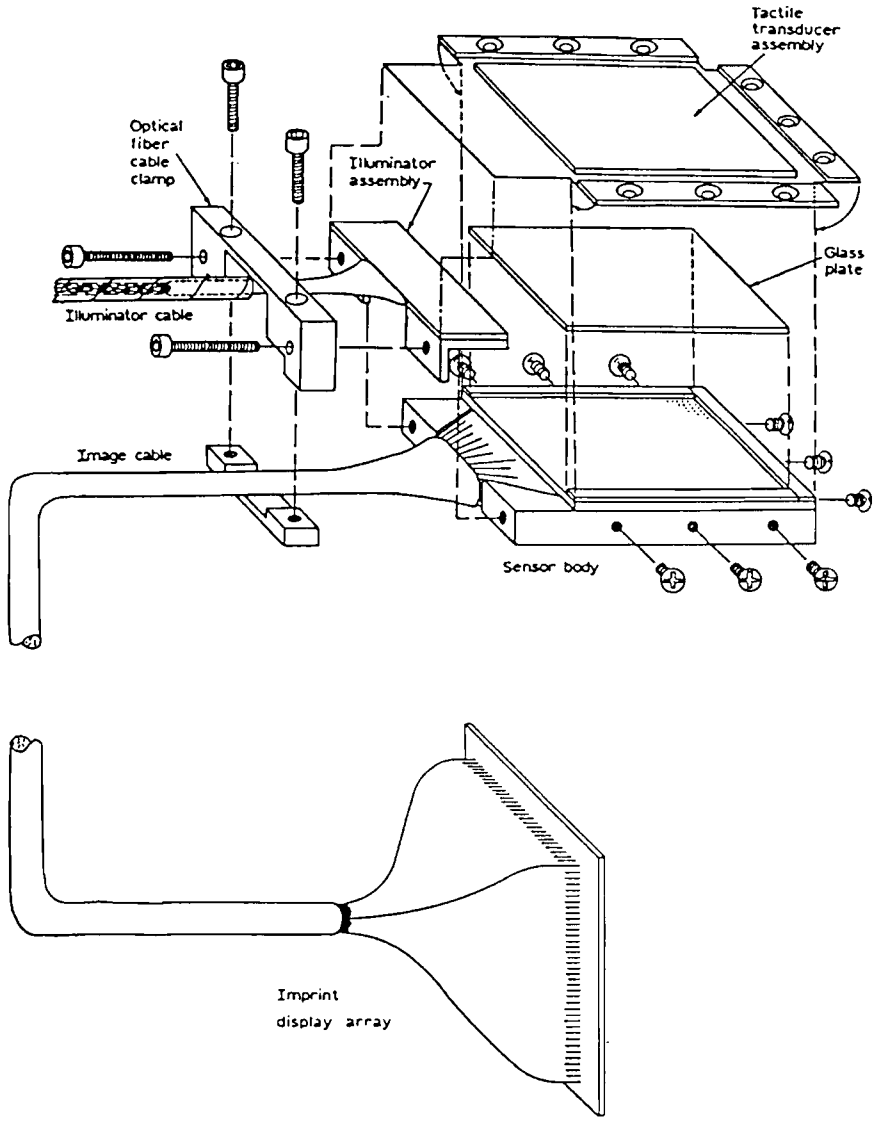

FIGURE 3: Planar, fiberoptic, TIR tactile sensor containing an array of 32 x 32 pressure sensing sites (1024 total) spaced 1 mm apart. From Begej [1985].

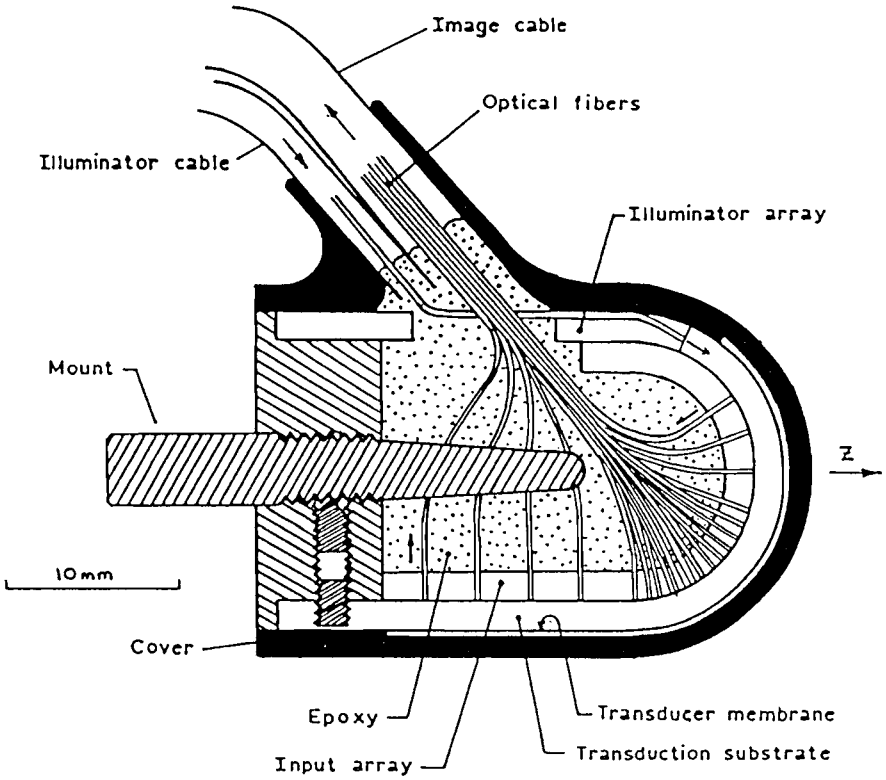

FIGURE 4: Internal construction of a fingertip-shaped fiberoptic tactile sensor. An arboreal distribution of optical fibers was used to acquire the optical pressure signals from the sensing surface and convey them to a remote camera for capture and processing. From Begej [1986, 1988a, 1988b].

This background of experience in fiberoptic FTIR pressure sensors was used as a starting point in the design and development of a full-length, flexible esophageal pressure sensor. Section 2.1.2 describes the first phase of the sensor development effort in which a design of a flexible sensor was pursued. This goal was not entirely achieved, and Section 2.1.3 describes the second development phase in which sensor flexibility was abandoned. Instead, a full-length but rigid sensor was designed and fabricated to partially prove the concept and to enable development and evaluation of the data processing and display elements of this program.

2.1.2. Flexible Sensor Development

The starting point in the design of a flexible esophageal pressure sensor is shown in Figure 5. The circumferential sensor design for sphincter pressure measurements was identical except that fibers were both linearly and circumferentially distributed. The sensor would be covered with a thin rubber sheath intended to act as an impermeable barrier between the interior of the sensor and the esophagus. This pneumatic barrier would be maintained along the sensor cables to the illuminator and camera interface points external to the body, thereby enabling the measurement of pressure relative to the ambient pressure external to the patient. Immediately inside the outer cover would be an aluminized mylar sheath covering a pressure transduction membrane of textured polyethylene. The mylar sheath would act as an light barrier to block the entrance of any ambient light filtering through the outer cover, and also as a reflector to minimize light losses from unsensorized portions of the waveguide.

In contrast to previous tactile sensor designs in which rigid waveguides were utilized (see Section 2.1.1), measurement of esophageal pressures required a flexible sensor, and therefore the use of a flexible waveguide. A tubular waveguide configuration was chosen as this corresponded to the geometry of the commercially-available materials suitable for use as waveguides. The sensing fibers would all be routed through the core of a flexible optical fiber substrate tube, the latter being optically isolated from the outer waveguide by a layer of aluminized mylar. The fibers in the core would be embedded in a silicone matrix to prevent self-abrasion and to provide mechanical support against collapse due to external pressures on the sensor.

Specification of sensor dimensions began with consideration of the minimum optical fiber size that could be employed. Preliminary routing and adhesion tests performed with 76 um diameter acrylic fiber (PolyOptics Corp.) revealed that this size was very difficult to handle in long lengths due to floating and charging by static electricity. The next size available, 127 um, was then tested with satisfactory results. With the fiber size selected, the minimum core diameter to support the passage of at least 256 fibers (the maximum number of sites the sensor would have) was determined to be 2.35 mm.

Selection of flexible waveguide and fiber substrate materials was restricted to commercially-available substances fabricated into a tubular geometry. A variety of such materials were procured for evaluation, e.g., polyurethane, vinyl, latex, silicone, Viton, and Norprene rubber. The minimum internal diameter of the fiber substrate was

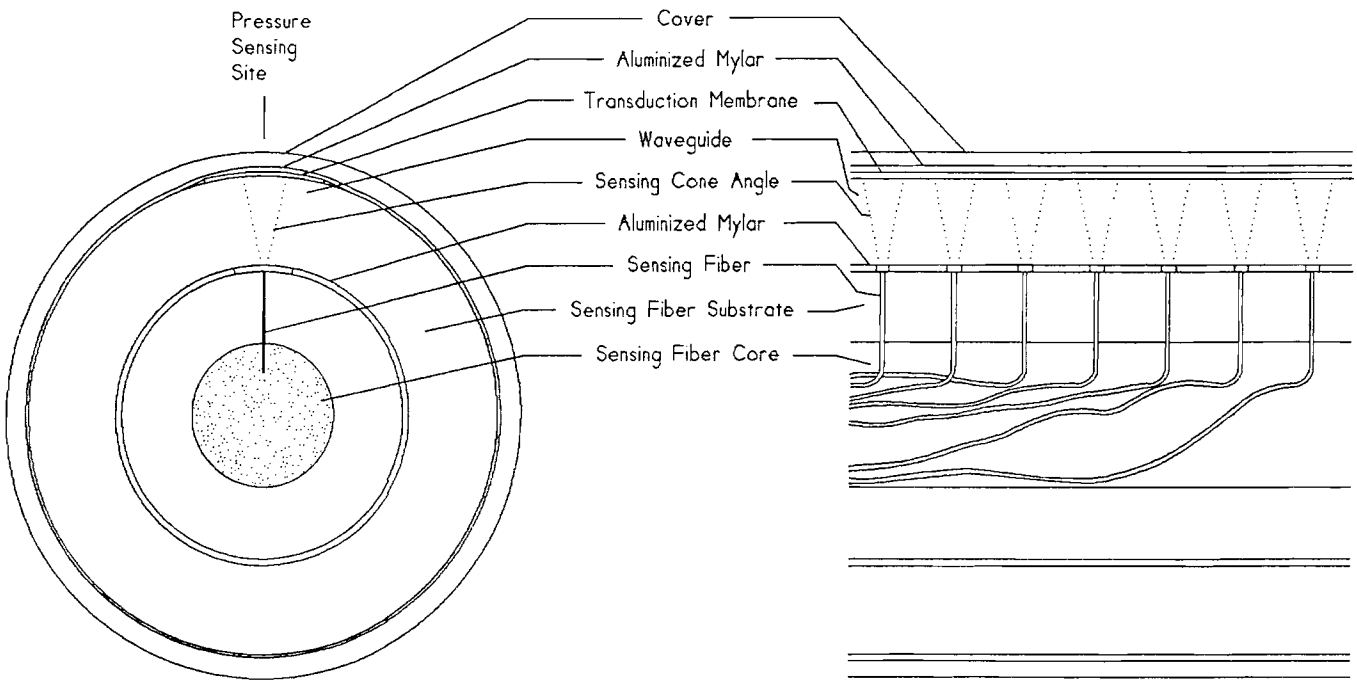

FIGURE 5: Design used as a starting point in the development of a flexible FTIR pressure sensor for this program. Only the linear section for esophageal measurements is shown. The sensor for sphincter pressures would be very similar, though with an added circumferential distribution of sensor sites.

maintained at 2.5 mm, with a wall thickness of at least 1 mm. This, in turn, dictated that the minimum internal diameter of the waveguide material be approximately 5 mm (allowing 0.5 mm for the aluminized mylar optical insulation), and the outer diameter approximately 7 to 9 mm.

The procedure for evaluating optical transparency of the various waveguide candidates (e.g., polyurethanes and vinyls) consisted in cutting a segment approximately 300 mm long, injecting light from a 150 W light source into one end, and qualitatively examining the amount of light emanating from the opposite end. The results from these tests proved to be very discouraging as in most cases only a faint glow emerged, an amount that was judged wholly inadequate considering the additional light losses that would be incurred transducing and conveying the pressure signal back to the CCD camera. After further searching and evaluations, the best results were obtained with a high-purity, surgical-grade polyurethane tubing (Tygon S-50-HL manufactured by the Norton Company). However, even in this case the maximum usable length was only 100 mm, less than half the length actually needed for a full-length esophageal pressure sensor.

In parallel with evaluations performed on the tubular waveguide materials, efforts were made to overcome the problem regarding the lack of waveguide transparency. One approach taken was to utilize high-transparency materials of higher stiffness. To this end, a tubular waveguide geometry was abandoned in favor of a simple cylinder or rectangular strip, as indicated in Figure 6. This permitted consideration of materials known to have a high transparency (e.g., acrylic, polycarbonate, butyrate, and glass), with the hope that waveguides made form these materials could be made sufficiently flexible by reducing their thickness to approximately 1 or 2 mm. Polycarbonate and butyrate strips were found to be insufficiently flexible or transparent, though their clarity was a significantly better than the tubing evaluated earlier. Glass strips were highly transparent, though far too rigid even when cut into a 1 x 1 mm square strip.

The most promising waveguide candidates were large diameter acrylic plastic optical fibers (Dupont, ESKA). Fibers measuring 1 mm diameter were more than adequately transparent, and were also sufficiently flexible for use in a first-generation esophageal sensor. However, two problems prevented satisfactory implementation of this approach. The first concerned attachment of the sensing fibers to the waveguide, and was eventually addressed by embedding the fibers in a thin substrate prior to bonding with the waveguide. A more difficult problem, however, was polishing the "top" surface of the waveguide to remove the fiber cladding and permit direct contact of the pressure transduction membrane with the core. Various scraping and

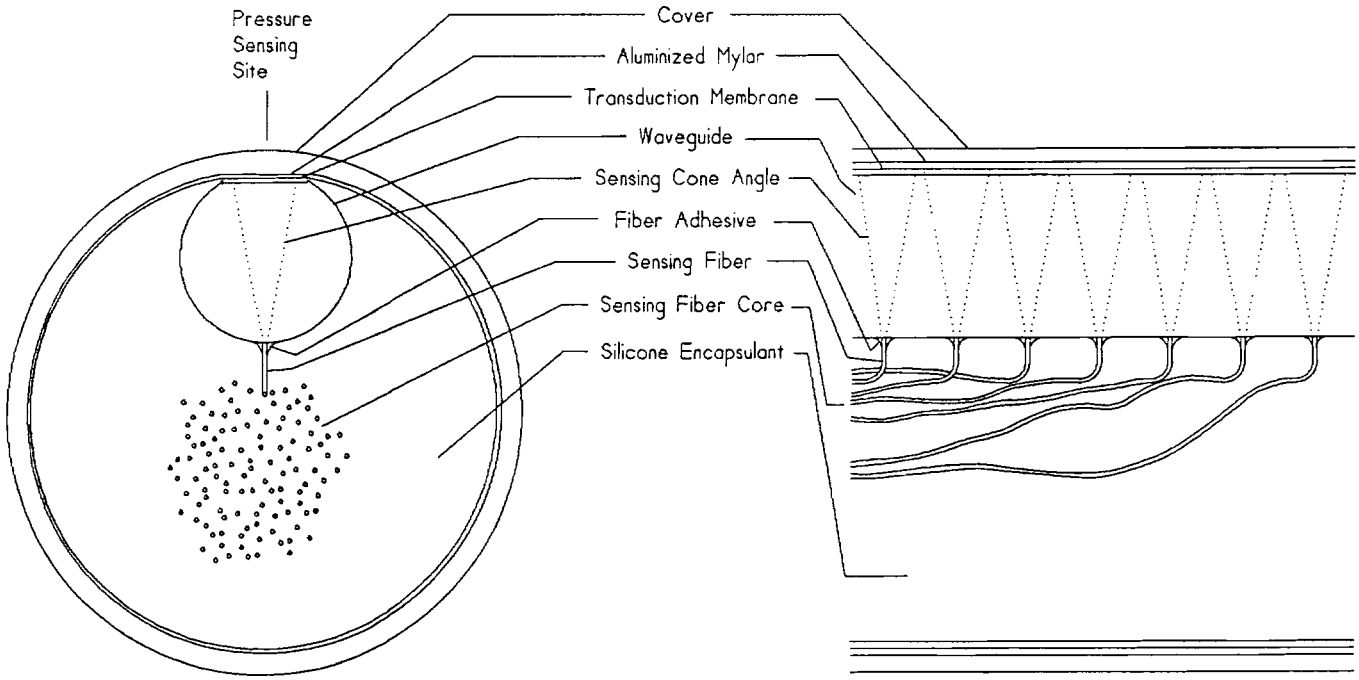

FIGURE 6: Alternative esophageal sensor design based upon the use of relatively stiff, highly-transparent waveguide materials that were flexible in thin sections. In this example, the sensor fibers were directly attached to an acrylic optical fiber.

polishing methods were explored, though none could selectively remove the cladding over the length needed for the esophageal pressure sensor. For this reasons, this approach was eventually abandoned.

Another approach considered in overcoming low waveguide transparency was to consider sensor designs in which light was injected uniformly along the length of the waveguide, rather than simply (and most conveniently) injecting the light at the proximal end. However, this approach was eventually abandoned for the fundamental reason that the light level provided from a single illumination fiber at each pressure sensing site was insufficient to generate a signal that could be reliably detected by the CCD camera.

2.1.3. Rigid Sensor Development

As summarized in the previous section, a significant effort was expended in trying to solve the problems of flexibility and transparency associated with the sensor waveguide. This effort was largely unsuccessful, and was eventually abandoned in favor of designing and fabricating a fully-functional rigid esophageal sensor that utilized a glass waveguide. This decision was made to permit other program tasks to proceed (e.g., development of a sphincter pressure sensor, and development of software for pressure sensor data acquisition, calibration, processing, and display), and to permit evaluation of the pressure monitoring system as a whole.

A diagram and photograph of the rigid sensor is shown in Figure 7 and 8, respectively. The sensor combined a long linear region for measuring esophageal pressures with a cylindrical sensor on the tip for characterizing circumferential (vector) sphincter pressures. This prototype had 101 and 88 sensor sites in the linear and cylindrical regions, respectively, for a total of 189 sites in the entire sensor. The site spacing in both the linear and circumferential directions was chosen to be approximately 2.5 mm. This spacing was dictated primarily by the available waveguide diameter, the desired length of the linear section, the length of the cylindrical sensor, and the number of circumferential sites. The values of these parameters were 8 mm, 250 mm, 25 mm, and 8 sites, respectively. (Had 12 circumferential sites been chosen, then the total number of sites in the sensor would have risen to 330, a far less manageable number than 189.)

The sensor design is very similar to the flexible sensor design previously shown in Figure 5, the most notable difference being the use of a rigid glass tube as the waveguide (4.6 mm ID x 7.1 mm OD) and the use of a semi-rigid slotted acrylic tube as the optical fiber substrate. This change in materials permitted the elimination of the reflective mylar film between the sensing fiber substrate tube and waveguide tube. Such a film was found to be unnecessary, as contact between the acrylic fiber substrate and the hard glass waveguide resulted in negligible light losses. However, the reflective film located between the waveguide and silicone rubber cover was retained, as the silicone caused heavy light losses when it touched and adhered to the waveguide.

Fabrication of the acrylic substrate for the sensor fibers was accomplished in a stepwise method beginning with the preparation of short segments measuring approximately 3.0 mm ID x 4.5 mm OD x 40 mm long. Those segments intended for use in the esophageal portion of the sensor had a linear

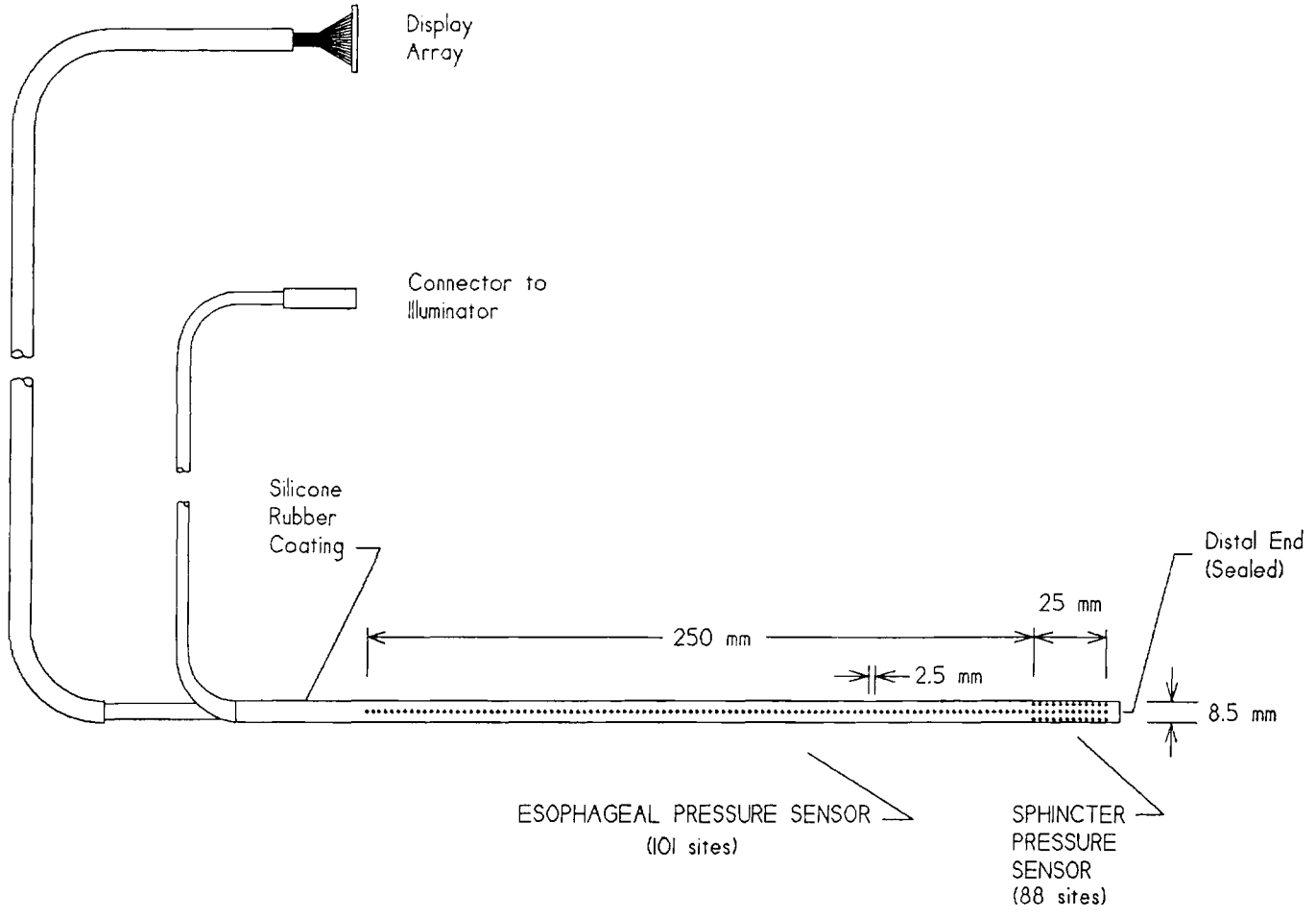

FIGURE 7: Diagram of the rigid esophageal and sphincter pressure sensor developed under this program. The body contained a linear sensor for measuring esophageal peristaltic wave pressures, whereas the tip contained a cylindrical sensor for measuring vector pressures within sphincters. The indices of the esophageal sensor sites range from 1 to 101 starting at the proximal end, whereas the indices of the cylindrical sensor range from (longitudinal index, circumferential index) = (1,1) to (11,8).

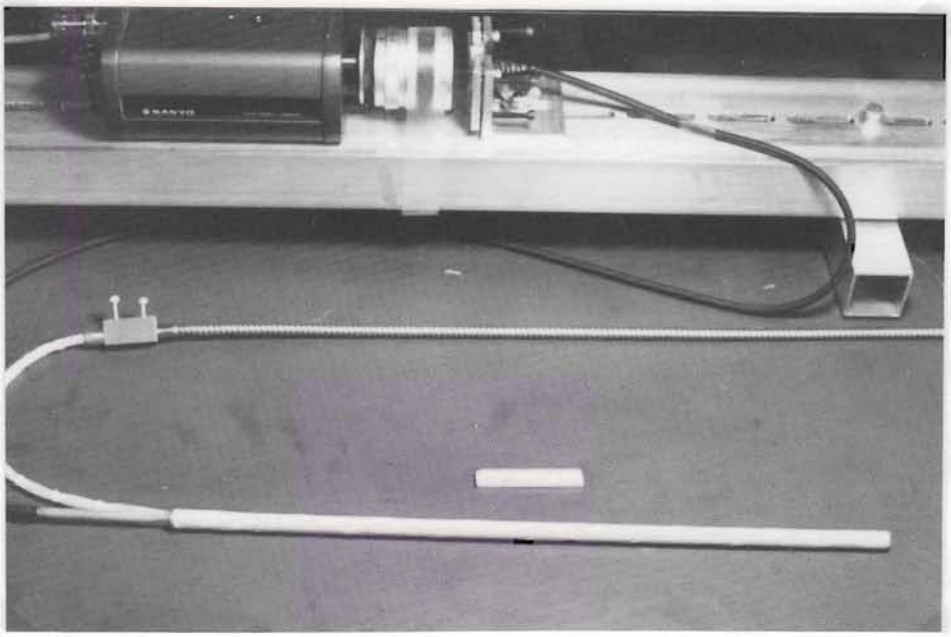

FIGURE 8: Rigid esophageal pressure sensor developed under this program (see previous figure for dimensions). Also shown at the top is the CCD camera interfaced to the sensor display array.

array of holes drilled with a size 80 carbide bit (304 um diameter). The segments were then longitudinally slotted on the wall opposite the fiber holes to permit threading of the optical fibers. All the linear sensor segments were then bonded together with acrylic cement. Only one segment was required for the sphincter portion of the pressure sensor, and it was drilled with the same bit while the sensor was mounted on a rotary indexer.

The first segment to be threaded with optical sensor fibers was the sphincter segment. Each 127 um diameter fiber was threaded from outside to inside starting at the distal end of the segment. The tip of each fiber was slightly bent to facilitate guidance down the segment. After threading was completed, the tube segment was filled under pneumatic pressure with epoxy (Devcon S-33, 30 minute cure time) to encapsulate the fibers within their holes and tube core. After curing, the excess fibers were trimmed off with a sharp razor blade, producing a clean optical finish on the severed fiber end. A photograph showing the appearance of the sphincter sensor segment prior to trimming of the fibers in shown in Figure 9.

Threading of the linear fiber substrate segments also began at the distal end. After all fibers were threaded, they were potted into their holes with epoxy (Devcon S-206, 5 minute cure time). A photograph of the sensor fiber substrate at this stage is shown in Figure 10. The protruding fiber ends were trimmed, and the linear portion of the sensor attached with acrylic cement to the previously fabricated cylindrical segment. After the fibers were folded down into the core, they were encapsulated with epoxy (Devcon S-33, 30 minute cure). A photograph of the finished fiber substrate is shown in Figure 11.

To facilitate viewing of the fiber ends with a CCD camera, the fibers from the sensor were embedded in a flat display array with the format shown in Figure 12. The fibers associated with esophageal and sphincter portions of the sensor were located in the upper and lower sectors of the array, respectively. The display array was fabricated from acrylic plastic (to facilitate drilling), and was threaded after the sensor substrate was completed (see Figure 11). Identification of the fibers was accomplished by illuminating the fiber end exposed at the sensor substrate, and selecting the corresponding illuminated fiber from the bundle at the opposite end. The display array before and after fiber encapsulation and trimming is shown in Figure 13.

Figure 14 shows the illumination collar in the process of being attached to the sensor. This device consisted of approximately 300 acrylic optical fibers (254 um diameter) arranged in an annulus and pressed against the proximal end of the waveguide. The input end of the illumination bundle

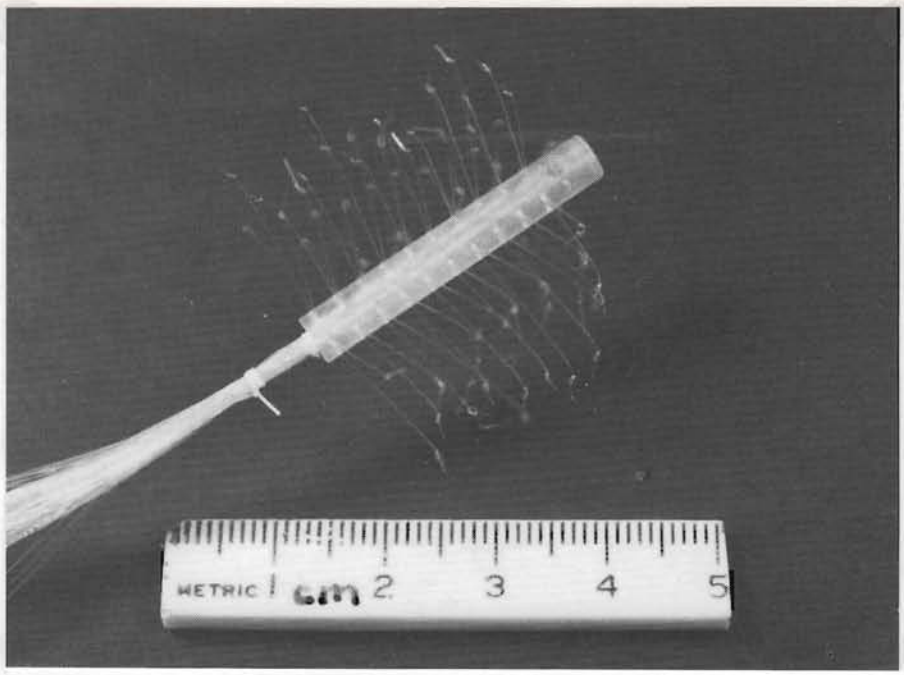

FIGURE 9: Appearance of the fiber substrate tube for the sphincter portion of the sensor after fiber threading, but before epoxy encapsulation and fiber trimming.

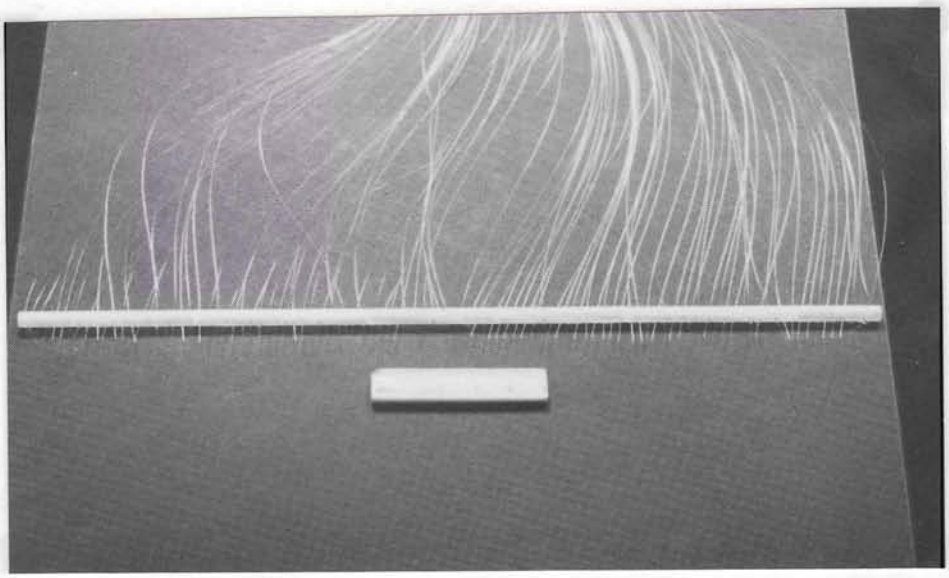

FIGURE 10: Optical sensor fibers (101 total) threaded through the linear fiber substrate. Fibers have been potted into their holes, but not fully trimmed or encapsulated into the substrate core.

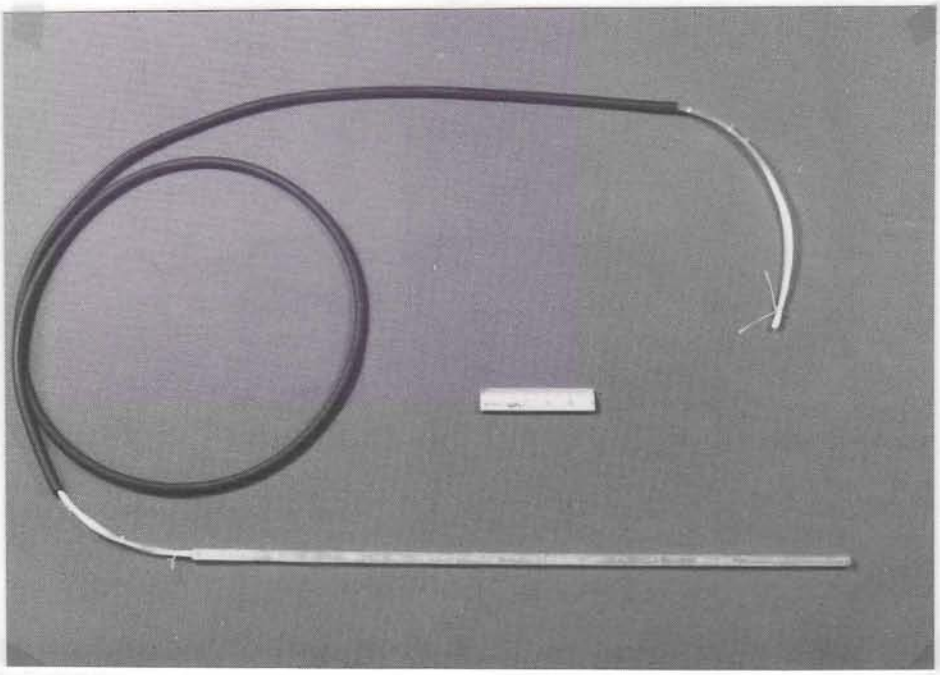

FIGURE 11: Finished sensor fiber substrate (bottom). The left and right sides contain the linear and cylindrical sensor fibers with 101 and 88 sites, respectively. The fiber cable is shown covered with a flexible Viton rubber sheath for protection against dust and abrasion damage.

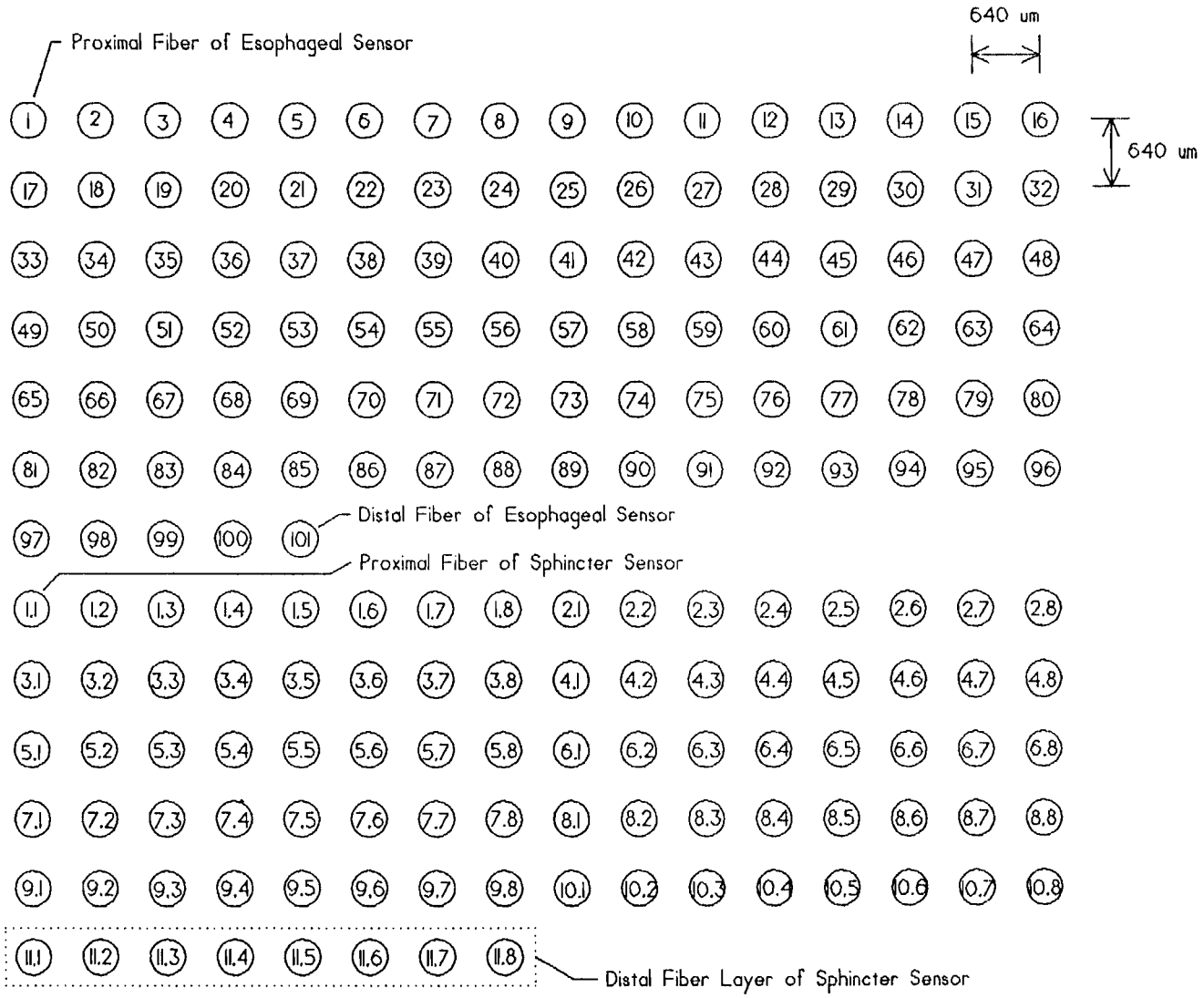

FIGURE 12: Arrangement of sensor fibers in the display array imaged by CCD camera. Top portion contains fibers from esophageal (linear) sensor region, with the proximal fiber located at the top-left corner. Bottom region contains fibers from sphincter (cylindrical) sensor region, with proximal layer located at center-left. See Figure 7 for corresponding fiber locations on sensor surface.

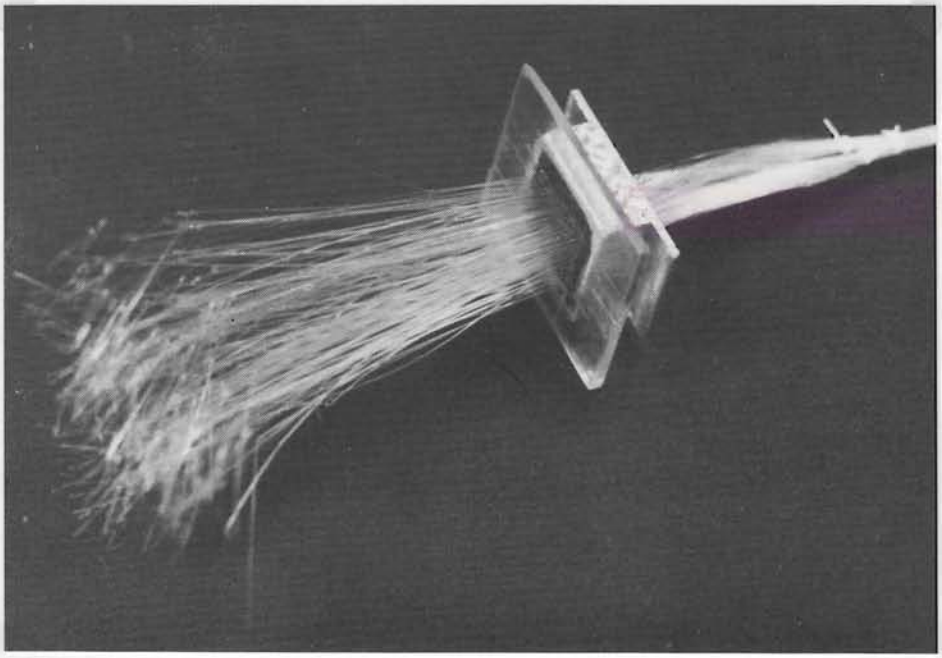

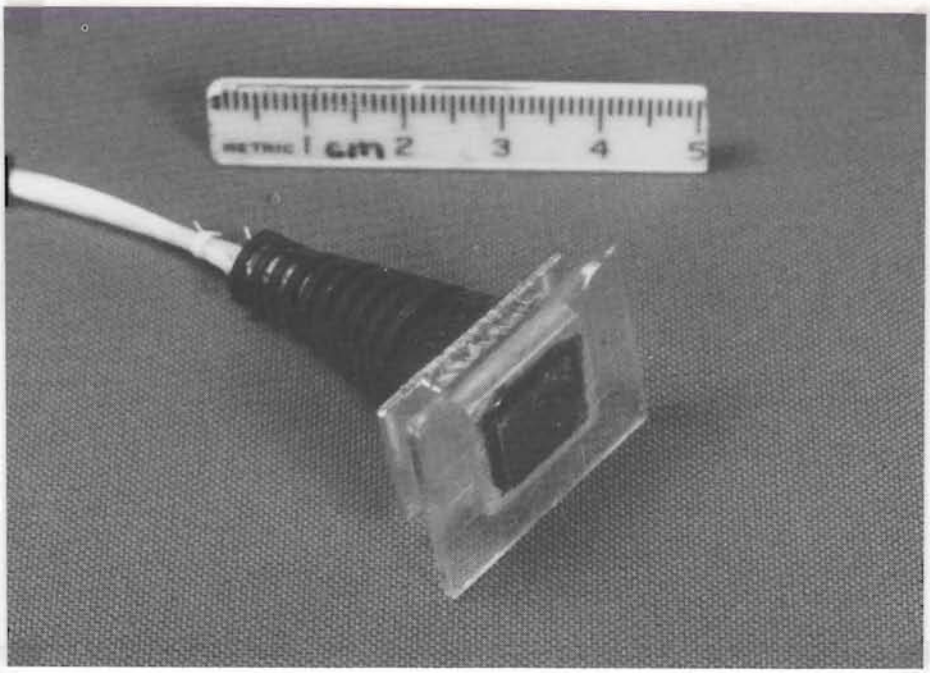

FIGURE 13: Sensor fiber display array shown before (top) and after (bottom) fiber encapsulation and termination.

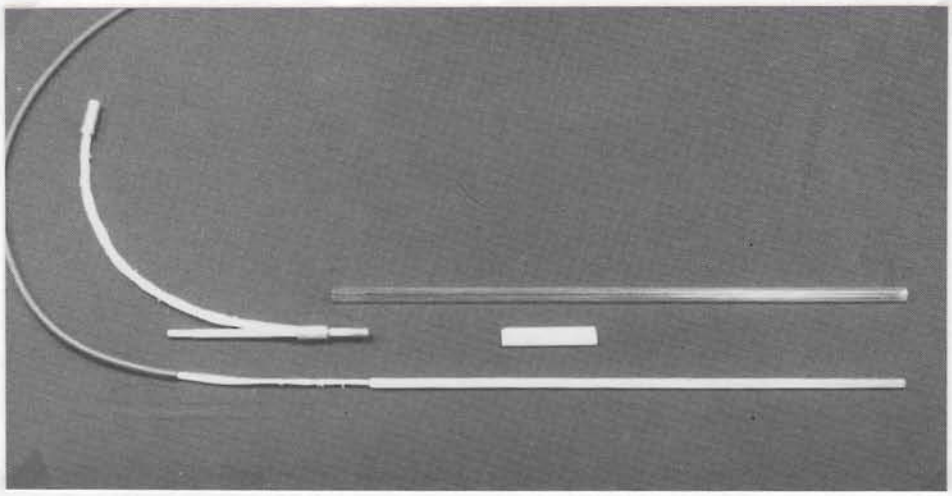

FIGURE 14: Illumination collar (center-left) for the rigid pressure sensor. The glass waveguide tube and completed sensor fiber substrate are also shown at the upper and lower portions of the photograph, respectively.

was terminated in a brass tube, and attached via an intermediate illumination cable to a 150 W fiberoptic illuminator. Reflective aluminum foil was bonded to the distal end of the waveguide to enhance the light level in the waveguide by reflecting light back into the waveguide that would otherwise be lost. The assembled sensor prior to covering is shown in Figure 15.

The final steps in sensor fabrication were attachment of the pressure transduction membrane and covering the sensor. The transduction membrane was made from white polyethylene film 89 um thick, and textured on the waveguide side by light abrasion with 200 grit sandpaper. This material was selected as past studies (Begej [1984] and [1986]) have proven this to be the most effective with regard to minimizing hysteresis and maximizing signal output. The transduction membrane was applied to only those portions of the waveguide monitored by sensor fibers, the balance of the waveguide area being covered with reflective mylar film. After application of the membrane, the sensor was spiral-wrapped with self-fusing silicone rubber tape (Scotch/3M No. 70) 280 um thick. Finally, a silicone end cap was attached to complete the pneumatic seal between the interior and exterior of the sensor.

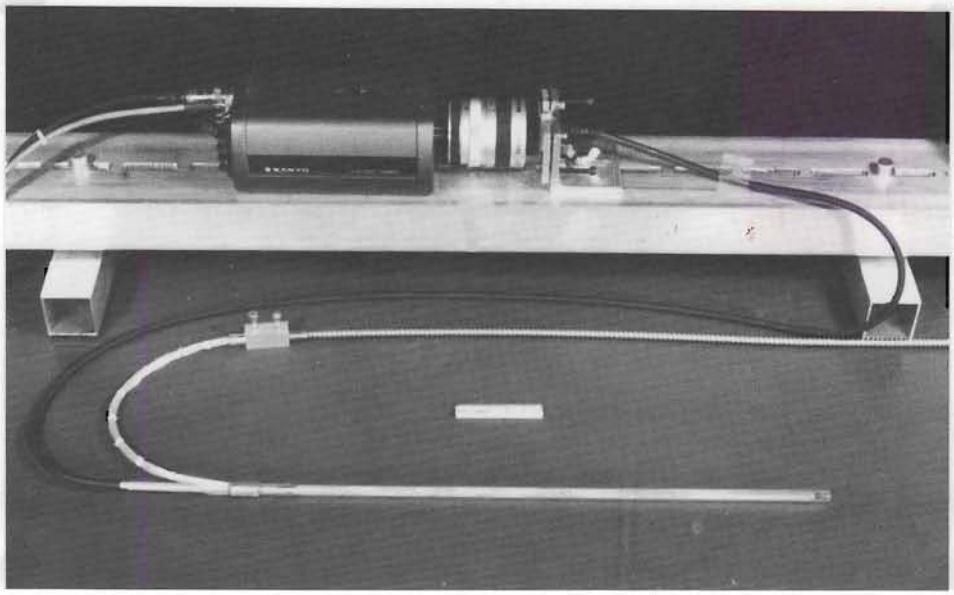

FIGURE 15: Assembled rigid pressure sensor prior to attachment of the sensor cover.

At the completion of sensor fabrication, a pressure chamber was also built to enable calibration of the sensor. This device is shown in Figure 16, and consisted of a 12.7 mm ID tube closed at one end and provided with a compressive O-ring seal at the other. Pressurization was accomplished by an electromechanical valve operated by a toggle switch.

Some typical sensor pressure response data obtained using the calibration device (and the software described in later sections) is shown in Figure 17. The following observations were made with respect to this data:

1. The pressure sensitivity range of the sensor is approximately 0 - 3,000 mmHg and, as such, is approximately 15 times higher than the pressures of interest in esophageal or sphincter pressure measurements (approx. 0 to 200 mmHg).

2. The shape of the pressure response curves is non-linear. Though pressure measurements beyond 3,000 mmHg were possible, such measurements were not in the range of highest sensitivity.

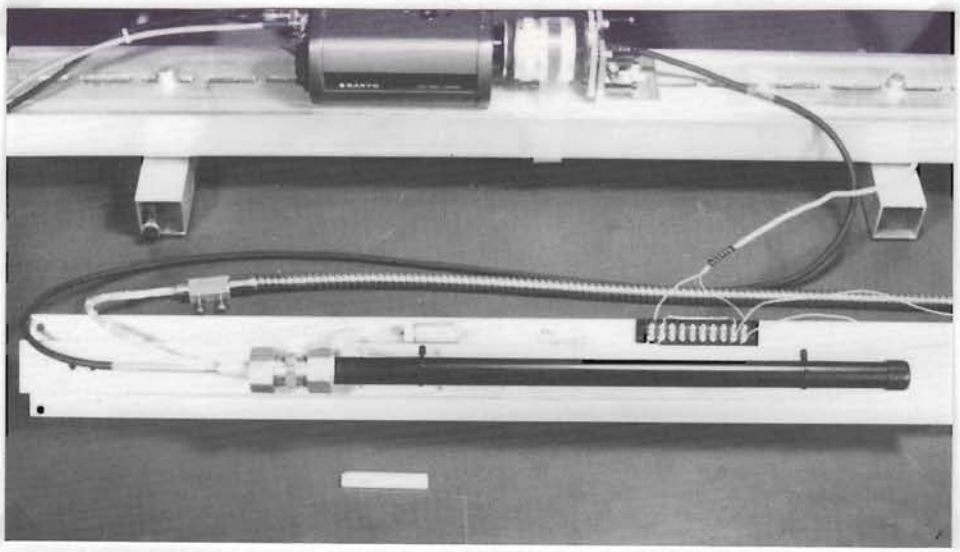

FIGURE 16: Pressurization chamber used to calibrate the esophageal pressure sensor. The right end of the tube was closed, and the left end provided with an O-ring seal which clamped onto the sensor at the proximal end. Air at a regulated pressure was admitted to the chamber by means of an electromagnetic valve.

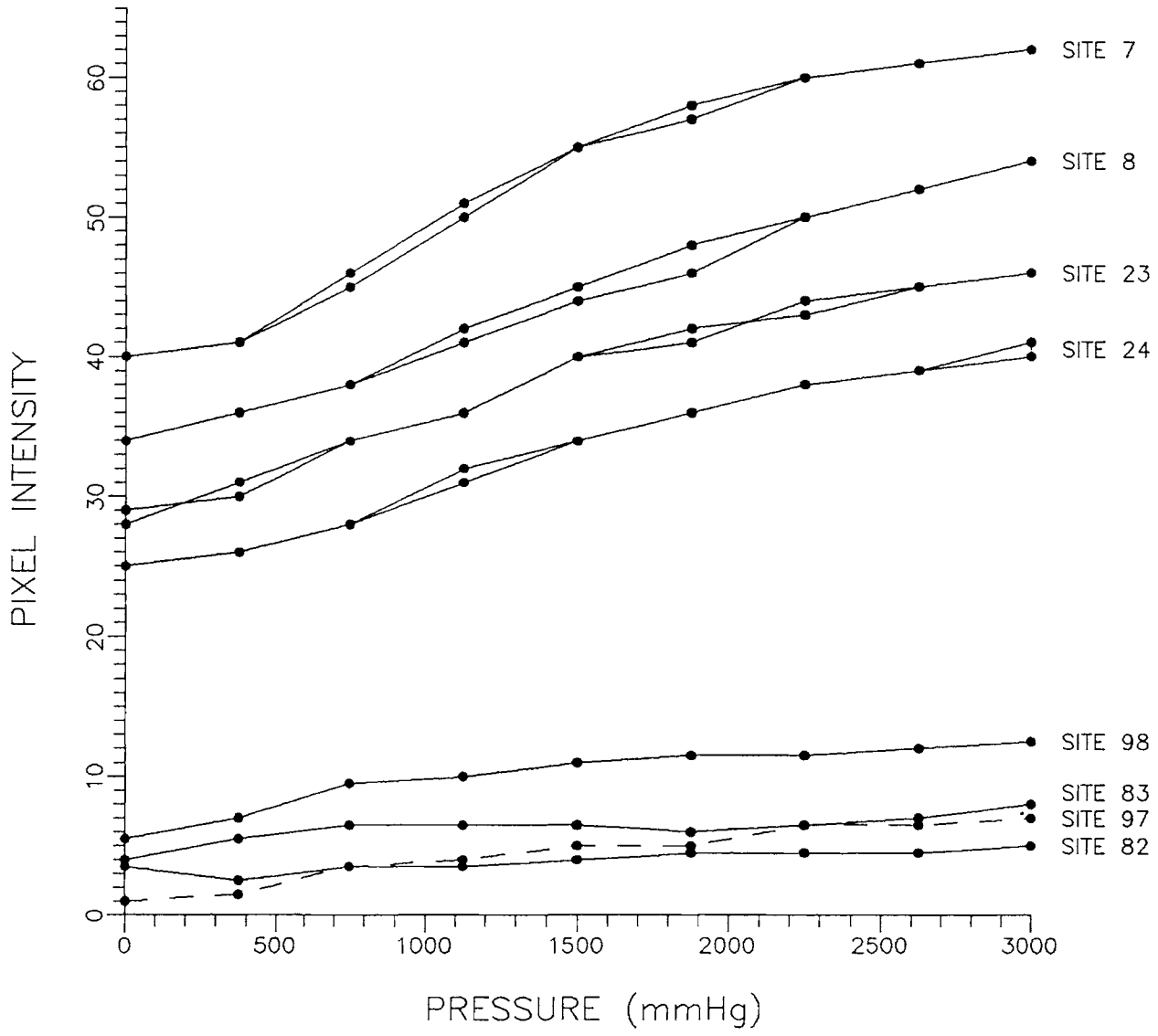

FIGURE 17: Representative pressure response of various sensor sites on the esophageal (linear) portion of the sensor. Top four curves show pressure data for increasing and decreasing pressure, whereas the pressure values have been averaged in the lower four curves.

3. The sensor signal intensity is seen to decrease as the location of the pressure site moves away from the light injection point at the proximal end of the waveguide, and is reduced to approximately 10% of the value at the proximal end. This is attributed to absorbtion or other losses associated with light transmission down the waveguide. A consequence of this effect is that the distal sites are expected to be far more susceptible to noise than proximal pressure sites.

4. There is a pronounced recovery of the signal as the distal end is approached, and is hypothesized to be caused by back-reflections from the reflector at the end of the waveguide.

2.2. Software Development

In addition to development of the sensor hardware, a parallel effort was also undertaken to develop software necessary to acquire, calibrate, process, and display the pressure data produced by the sensor. The initial plan for the software development effort entailed writing an integrated package which performed all these functions. However, due to time constraints imposed by difficulties encountered during sensor hardware development, this plan was modified to include only the development of code for data acquisition, calibration, and processing, while relying upon a commercially-available package called SURFER (Golden Software) for data display. This decision precluded the development of a system that might run in real time, though this compromise was deemed acceptable for a Phase I effort whose prime purpose was to demonstrate system feasibility.

The starting point for development of data acquisition, calibration, and processing software was a previously-written in-house C-code package for data acquisition from a video source. This menu-driven package was extensively modified and augmented to perform the functions needed by this project. The resultant data acquisition program consisted of the following modules:

MODULE NAME	MODULE SIZE Bytes	Lines	FUNCTION
ps.c	4,376	20	Main program
ps_m000.c	11,514	262	Main menu
ps_m100.c	22,258	377	Imprint I/O (video)
ps_m110.c	14,843	339	Display array set-up
ps_m120.c	16,617	362	Sensor calibration
ps_m130.c	8,097	156	Data acquisition
ps_m140.c	14,753	294	Data display
ps_util.c	12,061	249	Utility functions
	104,519	2,059	

The structure of the data acquisition program is shown in Figure 18, and illustrates how all functions are accessed through menus. At the top level, the MAIN MENU provides access to sub-menus pertaining to video data I/O, definition and set-up of the fiber optic display array, sensor calibration, data acquisition, and data processing for subsequent display by the SURFER plotting package.

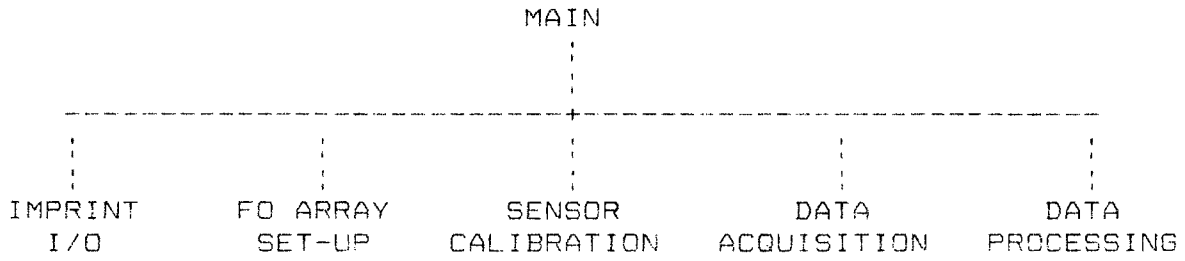

FIGURE 18: A hierarchical menu structure was used to control the acquisition, calibration, and processing of data from the pressure sensor.

The main menu display is shown in Figure 19. It illustrates the general format of the menus and how selections are made by entering item numbers. Selections (1) and (2) of each menu provide HELP and information regarding the current values or status of variables and file names, respectively. A print-out of the INFORMATION DISPLAY is shown in Figure 20.

The IMPRINT I/O menu shown in Figure 21 is a collection of important video image acquisition and interrogation functions. Though not directly utilized during pressure measurements, this menu was found to be quite useful during system development for such tasks as aligning the fiber optic display array with the CCD camera, adjustment of sensor signal intensity levels, and storing array images for future use. An example of such a display array image is shown in Figure 22 (refer to Section 2.1.3 and Figure 12 regarding format of the array indices).

Figure 23 shows the DISPLAY ARRAY DEFINITION menu which is used to define and save the locations of the maximum light signal from specific optical fibers in the image. This was accomplished by selection number (5) in which a cursor was superimposed on an image, such as the one shown in Figure 22. The user first specified the indices of the pressure sites to be defined (e.g., 1 to 101), and then moved the cursor about each site searching for the maximum intensity. Once found, that pixel location was entered and the program automatically requested that the user move from site to site until the entire array was defined. An example showing the display array definition for the 101 pressure sensing sites in the linear portion of the sensor is shown in Figure 24.

PRESSURE SENSOR SYSTEM MAIN MENU (No. 000)

1. Help
2. Information display

3. Restore previous data and files
4. Imprint I/O (100)
5. Define FO display array (110)
6. Sensor calibration (120)
7. Make a run (130)
8. Data display (140)
9. Change menus

99. Exit to DOS

FIGURE 19: Appearance of the MAIN MENU which allowed access to all functions pertaining to system operation. Items (1) and (2) provided on-line help and system parameter information, and were functions available on all menus.

INFORMATION DISPLAY

Number of taxels:	1
Number of scans:	1
Scan time (ms):	1
Cell size (pixels):	1
Maximum pres (mmHg):	0

Imprint file name:	CAMERA IMAGE
Array definition FN:	arraydef.xxx
Zero pres. inten FN:	sp_inten.xxx
Max pres. inten. FN:	mp_inten.xxx
Run pressure data FN:	run_pres.xxx
Data FN (SURFER dat):	ps_xxxx.dat
Data FN (SURFER grd):	psg_xxxx.grd

FIGURE 20: Knowledge of important parameters and file names were always available through the selection of menu item number 2. The above information display contains default values associated with system start-up.

IMPRINT INPUT/OUTPUT (No. 100)

1. Help
2. Information display

3. Display live imprint
4. Acquire imprint from camera
5. Recall imprint from disk
6. List imprint file directory
7. Place cursor on imprint
8. Print window centered on cursor
9. Save imprint

30. Change menus

FIGURE 21: The IMPRINT INPUT/OUTPUT menu was used to capture and manipulate image data from a CCD camera.

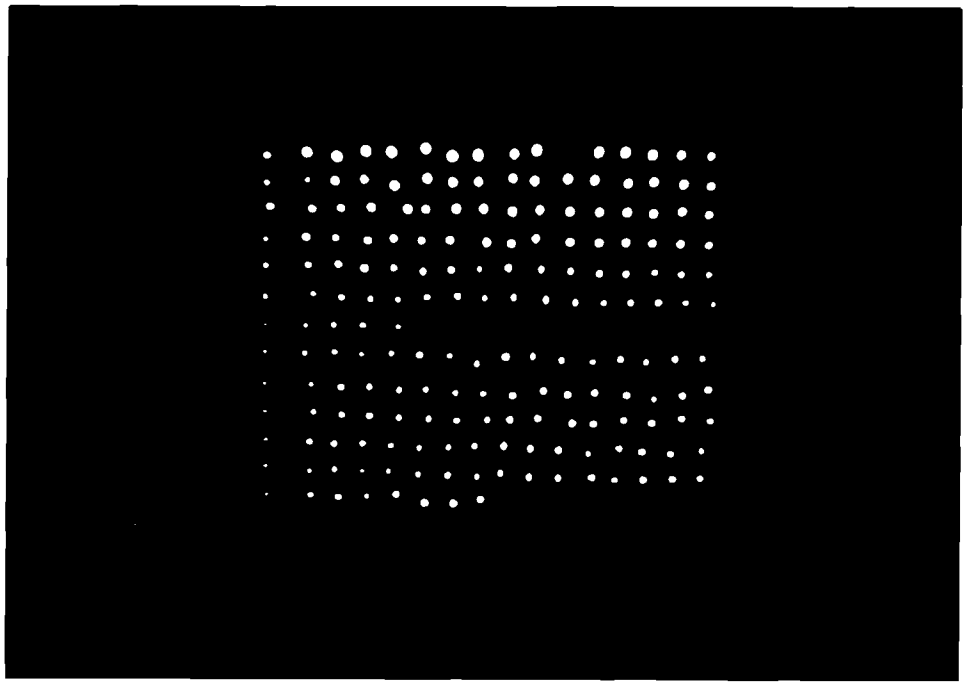

FIGURE 22: Image of sensor array re-displayed on a monitor after being captured by the CCD camera and saved to a file: refer to Figure 12 for array index definitions. Note that fibers located closest to the proximal (light injection) end of the sensor are the brightest. Also note the absence of fiber number 11 - it was accidentally severed during sensor assembly.

DISPLAY-ARRAY DEFINITION (No. 110)

1. Help
2. Information display

3. Recall FO array definition
4. List array definition file directory
5. Define display fiber locations in array
6. Save array definition
7. Print fiber locations (on monitor)
8. Display fiber locations (non-destructive)

99. Change menus

FIGURE 23: The DISPLAY ARRAY DEFINITION menu allowed specification of the locations in a camera image (e.g., see Figure 22) that correspond to the maximum light intensity emanating from the optical fibers.

FO array definition stored in file arraydef.007:

TAX	-X-	-Y-	TAX	-X-	-Y-	TAX	-X-	-Y-	TAX	-X-	-Y-	TAX	-X-	-Y-	TAX	-X-	-Y-
1	36	43	2	49	41	3	58	43	4	67	40	5	76	41	6	87	39
7	96	42	8	105	41	9	117	41	10	124	39	11	145	39	12	145	39
13	154	39	14	163	40	15	173	40	16	183	40	17	36	54	18	49	53
19	58	53	20	67	52	21	77	55	22	88	51	23	96	53	24	105	53
25	116	51	26	124	52	27	135	51	28	144	51	29	156	52	30	164	51
31	174	52	32	183	53	33	37	65	34	50	65	35	60	65	36	70	64
37	81	65	38	87	65	39	98	64	40	107	64	41	117	65	42	126	64
43	136	64	44	146	64	45	156	64	46	164	65	47	174	63	48	183	65
49	36	79	50	49	78	51	58	77	52	69	78	53	77	77	54	86	78
55	96	77	56	108	78	57	116	78	58	125	76	59	136	77	60	146	77
61	155	77	62	164	77	63	174	77	64	184	78	65	36	90	66	49	90
67	59	89	68	68	90	69	77	90	70	87	91	71	96	90	72	106	90
73	116	89	74	127	89	75	137	90	76	147	91	77	156	90	78	166	90
79	175	90	80	184	90	81	36	104	82	51	102	83	60	103	84	70	103
85	79	103	86	88	102	87	99	101	88	108	102	89	118	101	90	129	102
91	139	103	92	149	103	93	158	102	94	167	102	95	177	102	96	186	103
97	36	116	98	49	116	99	58	115	100	67	115	101	79	115	102	0	0
103	0	0	104	0	0	105	0	0	106	0	0	107	0	0	108	0	0
109	0	0	110	0	0	111	0	0	112	0	0	113	0	0	114	0	0
115	0	0	116	0	0	117	0	0	118	0	0	119	0	0	120	0	0
121	0	0	122	0	0	123	0	0	124	0	0	125	0	0	126	0	0
127	0	0	128	0	0	129	0	0	130	0	0	131	0	0	132	0	0

Hit ENTER key to continue

FIGURE 24: An example of a fiber optic array definition file in which the maximum light intensity locations associated with each optical fiber are defined in terms of the horizontal (X) and vertical (Y) pixel coordinates. This data corresponds to the first 101 fibers in array image shown in Figure 22. Note that the origin of the coordinate system is at the top-left of the screen, and that the pixel coordinate values range from (X,Y) = (0,0) to (255,255). Also note that damaged site number 11 was assigned the same coordinates as site 12, thereby causing the intensity data for these fibers to be identical.

Once the locations of intensity data in the video image were defined, the sensor could be calibrated. As illustrated in Figure 17, the response of the sensor to pressure was both non-linear and dependent on the pressure sensor site location. Sites located towards the distal end were found to produce signals that were far weaker than those located at the proximal end at which the illumination is injected. A complete sensor calibration under these circumstances would require calibration of each individual site over the full range of expected operating pressures. As such a full calibration would be both tedious and unnecessary in a system undergoing development, the non-linear behavior was deliberately ignored. For developmental and illustrational purposes it was assumed the sensor behavior was linear, and that it would be sufficient to determine only the zero and maximum pressure responses of each pressure site for calibration purposes. The pressure at each site, then, was simply calculated by linear interpolation between these two extreme values.

There was some unresolved concern at the start of this project with regard to the mechanical stability of the fiber display array with respect to the CCD camera. Permanent movements on the order of 25 um caused by bumps or jarring were thought to be sufficient to cause a change in calibration due to displacement of the maximal light intensity away from the pixel coordinate that had been associated with it. To address this potential problem, a decision was made to treat the array definition coordinates merely as starting points for a local search for the true light maxima. The search was confined to a square cell centered about each array definition point, with cell dimensions being user-specifiable, e.g., 1,3,5,... The cost of this approach was increased data processing time due to the search process. However, in the course of development during which the apparatus was subjected to various bumps and jarring, old and new array definitions were compared and found to be unchanged, indicating that no significant shifting was occurring and that cell-searching would not need to be incorporated in future versions of this system.

The sensor calibration menu is shown in Figure 25. Calibration was performed by inserting the sensor into the pressure calibration device (see Figure 16), capturing data images (using the menu shown in Figure 21) at the minimum and maximum pressures, and selecting function number (4) to extract the minimum and maximum intensity values at the defined array locations. An example of the data in the calibration files is shown in Figure 26 (note that the search cell size was 3).

SENSOR CALIBRATION (No. 120)

1. Help
2. Information display

3. Define maximum pressure
4. Acquire calib data from current imprint
5. List calibration file directory
6. Recall calibration data from disk
7. Save calibration data to disk
8. Print calibration data

98. Change menus

FIGURE 25: Once the fiber array had been defined, the sensor could be calibrated utilizing the above menu. The response of each pressure sensor site was presumed to be linear between zero and some maximum working pressure, thus requiring data at only two pressures.

The menu for making a run is shown in Figure 27. The most important system parameters could be set or changed in this menu, which included the number of pressure sensor sites, the number of scans in a run (typically 50), the time between each scan, the search cell size, and the maximum pressure used during calibration. Once these parameters were entered, the fiber array defined, and calibration files specified, then selection number (7) would execute a run, i.e., acquire images, extract data, and compute the pressures.

Once the data was acquired and pressures computed, the DATA DISPLAY menu shown in Figure 2.2-28 was used to format the data for display by a commercial three-dimensional plotting program called SURFER. In most cases, it was found most convenient to choose the .grd format as it minimized the file size and time required to plot the data.

zp_inten.008 { CAMERA IMAGE arraydef.007 cell size = 3 }

TAX	INT	TAX	INT	TAX	INT	TAX	INT	TAX	INT	TAX	INT	TAX	INT	TAX	INT
1	14	2	24	3	30	4	27	5	31	6	33	7	38	8	30
9	25	10	33	11	31	12	31	13	34	14	28	15	26	16	22
17	10	18	8	19	21	20	19	21	26	22	28	23	30	24	24
25	22	26	31	27	30	28	28	29	19	30	25	31	26	32	16
33	15	34	15	35	16	36	18	37	23	38	18	39	24	40	27
41	23	42	24	43	25	44	25	45	21	46	20	47	21	48	19
49	9	50	17	51	13	52	16	53	23	54	19	55	21	56	27
57	18	58	22	59	20	60	21	61	19	62	18	63	20	64	14
65	9	66	8	67	18	68	18	69	13	70	16	71	14	72	8
73	16	74	15	75	16	76	16	77	15	78	7	79	11	80	11
81	8	82	6	83	9	84	9	85	9	86	10	87	10	88	12
89	13	90	15	91	16	92	9	93	12	94	13	95	6	96	6
97	3	98	4	99	9	100	6	101	7	102	0	103	0	104	0
105	0	106	0	107	0	108	0	109	0	110	0	111	0	112	0
113	0	114	0	115	0	116	0	117	0	118	0	119	0	120	0
121	0	122	0	123	0	124	0	125	0	126	0	127	0	128	0
129	0	130	0	131	0	132	0	133	0	134	0	135	0	136	0
137	0	138	0	139	0	140	0	141	0	142	0	143	0	144	0
145	0	146	0	147	0	148	0	149	0	150	0	151	0	152	0
153	0	154	0	155	0	156	0	157	0	158	0	159	0	160	0

mp_inten.008 { CAMERA IMAGE arraydef.007 cell size = 3 }

TAX	INT	TAX	INT	TAX	INT	TAX	INT	TAX	INT	TAX	INT	TAX	INT	TAX	INT
1	26	2	37	3	45	4	43	5	46	6	51	7	58	8	47
9	37	10	52	11	49	12	49	13	49	14	43	15	37	16	35
17	23	18	20	19	32	20	33	21	40	22	38	23	46	24	37
25	37	26	40	27	39	28	40	29	28	30	32	31	37	32	25
33	23	34	24	35	23	36	26	37	32	38	27	39	32	40	35
41	31	42	28	43	29	44	28	45	25	46	24	47	24	48	24
49	12	50	19	51	17	52	19	53	26	54	23	55	24	56	31
57	22	58	26	59	23	60	24	61	21	62	20	63	23	64	16
65	12	66	12	67	20	68	18	69	17	70	20	71	15	72	11
73	18	74	16	75	18	76	19	77	15	78	8	79	13	80	13
81	9	82	10	83	12	84	12	85	13	86	13	87	14	88	16
89	17	90	18	91	17	92	11	93	15	94	15	95	8	96	9
97	6	98	6	99	11	100	9	101	12	102	0	103	0	104	0
105	0	106	0	107	0	108	0	109	0	110	0	111	0	112	0
113	0	114	0	115	0	116	0	117	0	118	0	119	0	120	0
121	0	122	0	123	0	124	0	125	0	126	0	127	0	128	0
129	0	130	0	131	0	132	0	133	0	134	0	135	0	136	0
137	0	138	0	139	0	140	0	141	0	142	0	143	0	144	0
145	0	146	0	147	0	148	0	149	0	150	0	151	0	152	0
153	0	154	0	155	0	156	0	157	0	158	0	159	0	160	0

FIGURE 26: The calibration procedure generated two data files containing the maximum light intensities associated with each fiber at zero and maximum intensities (shown in the top and bottom tables, respectively). Only data for the 101 pressure sensor sites in the linear portion of the sensor are indicated in this example.

MAKE A RUN (No. 130)

1. Help
2. Information display

3. Define number of taxels
4. Define number of scans
5. Define scan time
6. Define cell size
7. Define maximum pressure
8. Make a run

99. Change menus

FIGURE 27: Menu for making a run. The basic parameters regarding the number of sensor sites, number of scans, scan time, search cell size, and maximum calibration pressure could be entered or changed in this menu.

DATA DISPLAY (No. 140)

1. Help
2. Information display

3. List run directory
4. Save data to SURFER .dat file
5. Save data to SURFER .grd file
6. Print pressure data for single scan

99. Change menu

FIGURE 28: This menu was used primarily to format the pressure data after a run for subsequent passage to a commercial three-dimensional plotting program called SURFER. Single-scan pressure data could also be displayed for development purposes.

2.3. Sensor System Evaluation

The primary components of the esophageal pressure sensor system are shown in Figure 29, and consist of the sensor, sensor illuminator, a PC-XT with video digitizer for data acquisition, and a PC-AT with a color monitor for data display. The evaluation protocol consisted of testing the sensor performance in response to synthesized pressure waveforms representing the peristaltic wave action of the esophagus and the contractile behavior of a sphincter. No tests were performed in this Phase I study with live animal or human subjects.

The esophageal sensor was evaluated with the aid of the peristaltic wave synthesizer. This device consisted of a weighted, rubber-covered roller that was applied to the surface of the pressure sensor, and pulled at a uniform rate along its length to duplicate the progressive motion of a peristaltic wave. The mass of the roller and supplementary weight ranged from 500 - 1000 g, and was adjusted to provide reliable pressure readings for the entire length of the sensor (this required pressures far in excess of the calibrated value). The procedure for testing the linear portion of the sensor is outlined below:

1. Initialize the data acquisition system, i.e., enter the number of pressure sensing sites (101) and the number of scans (50).

2. Calibrate the sensor (using the device shown in Figure 16) at the minimum and maximum pressures of 0 and 2,625 mmHg, respectively.

3. Start the run.

4. Place the roller used to simulate esophageal contractions on the proximal end of the sensor.

5. Move the roller in the desired trajectory toward the distal end of the sensor.

6. Take the roller off the sensor just before the last scan occurs.

7. Process and save the data.

8. Return to Step (3) for the next run.

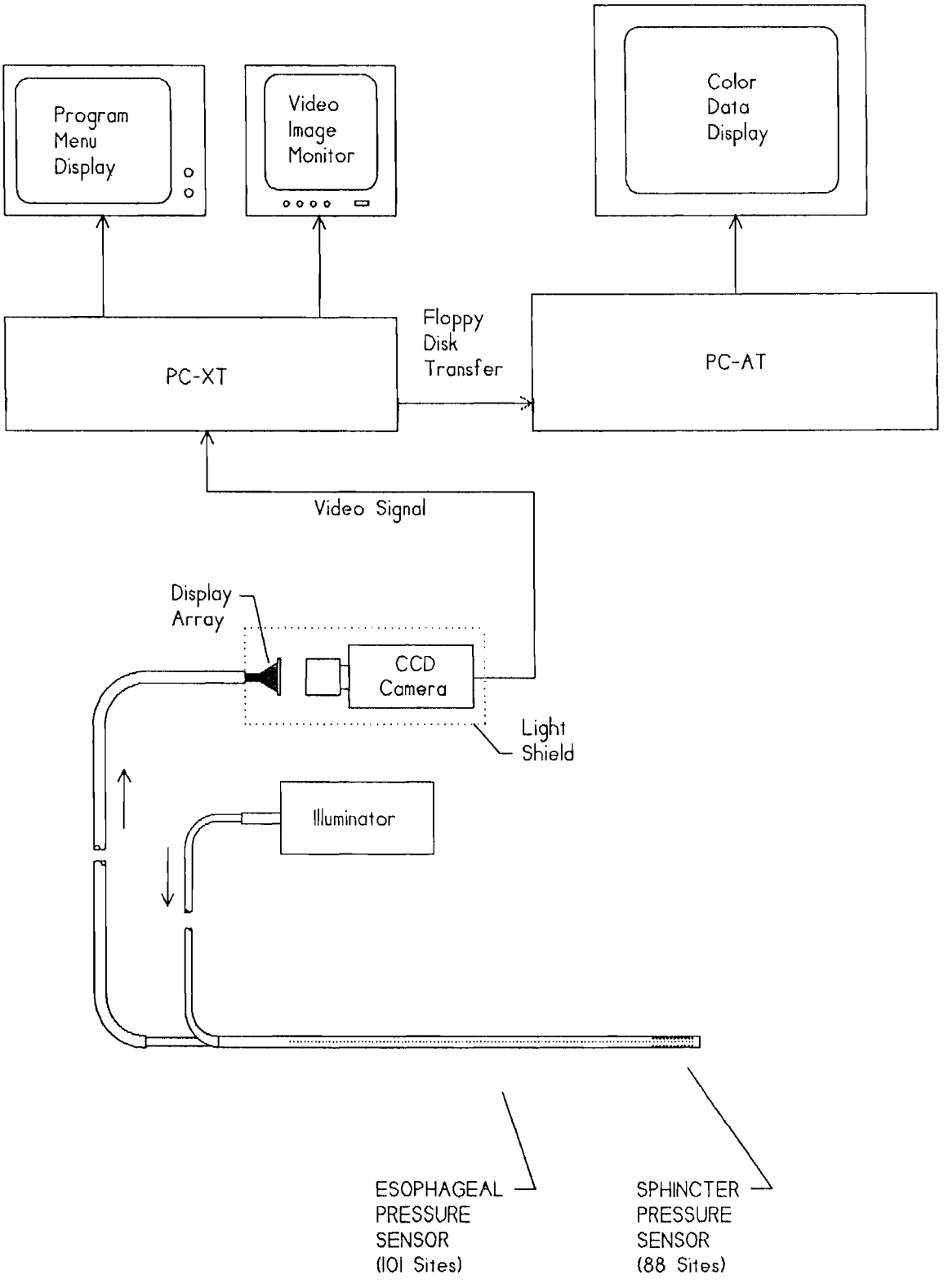

FIGURE 29: Principal components of the esophageal pressure monitor system assembled for evaluation. This "as built" system may be compared with the original concept shown in Figure 1.

As indicated in Figure 29, data acquisition and data display functions have been divided between two processors. After the data was collected and stored in a file, it was then transferred by floppy disk to a high-speed PC-AT equipped with a math co-processor and color display. The pressure data was then processed and displayed using the commercial plotting program SURFER (Golden Software Inc.) in a variety of 3-D formats.

For example, Figures 30, 31 and 32 show the pressure data for various simulated esophageal conditions displayed as 3-D surfaces. In each figure, the pressure surface was plotted as a function of the distance along the sensor (starting at the proximal end) and time (i.e., scan number). Figure 30 shows the appearance of a "normal" esophageal contraction in which the pressure wave moved at a uniform rate down the sensor. In contrast, Figures 31 and 32 illustrate the pathological conditions of retrograde and weak contractions, respectively.

A common feature to all these plots is the presence of increasing noise with distance along the sensor. This is a direct consequence of decreasing signal-to-noise ratio, as noted earlier in Section 2.1.3 and Figure 17. It was observed that some important details were difficult to extract from these plots, e.g., the linearity of a "normal" contraction wave, or the exact shape of the pressure ridge during retrograde contraction, or extraction of the main pressure waveform from noise at distant pressure site positions, or determination of pressure magnitudes. For these reasons, it was concluded that pressure surface plots were not entirely suitable for visualizing data in a clear and unambiguous manner.

The topographical format was also explored as a means of data presentation. Figures 33, 34 and 35 show the same pressure data previously presented in Figures 30, 31, and 32 regarding normal, retrograde, and weak peristaltic contractions, but now displayed in a colorized topographical plot. It is clear that this approach is much more successful at succinctly presenting the most pertinent data and suppressing the rest. The linearity of a normal contraction and the "switchbacking" of a retrograde contraction are readily seen in Figure 33 and 34, respectively, as is the gap in the pressure ridge associated with the weak contraction shown in Figure 35. It was concluded that the topographical method of data presentation combined with colorization of the levels was significantly superior to the surface plot method, and offered the best opportunity to formulate rapid diagnoses based upon the presentation of sensor data in a simple and intuitively- interpretable manner.

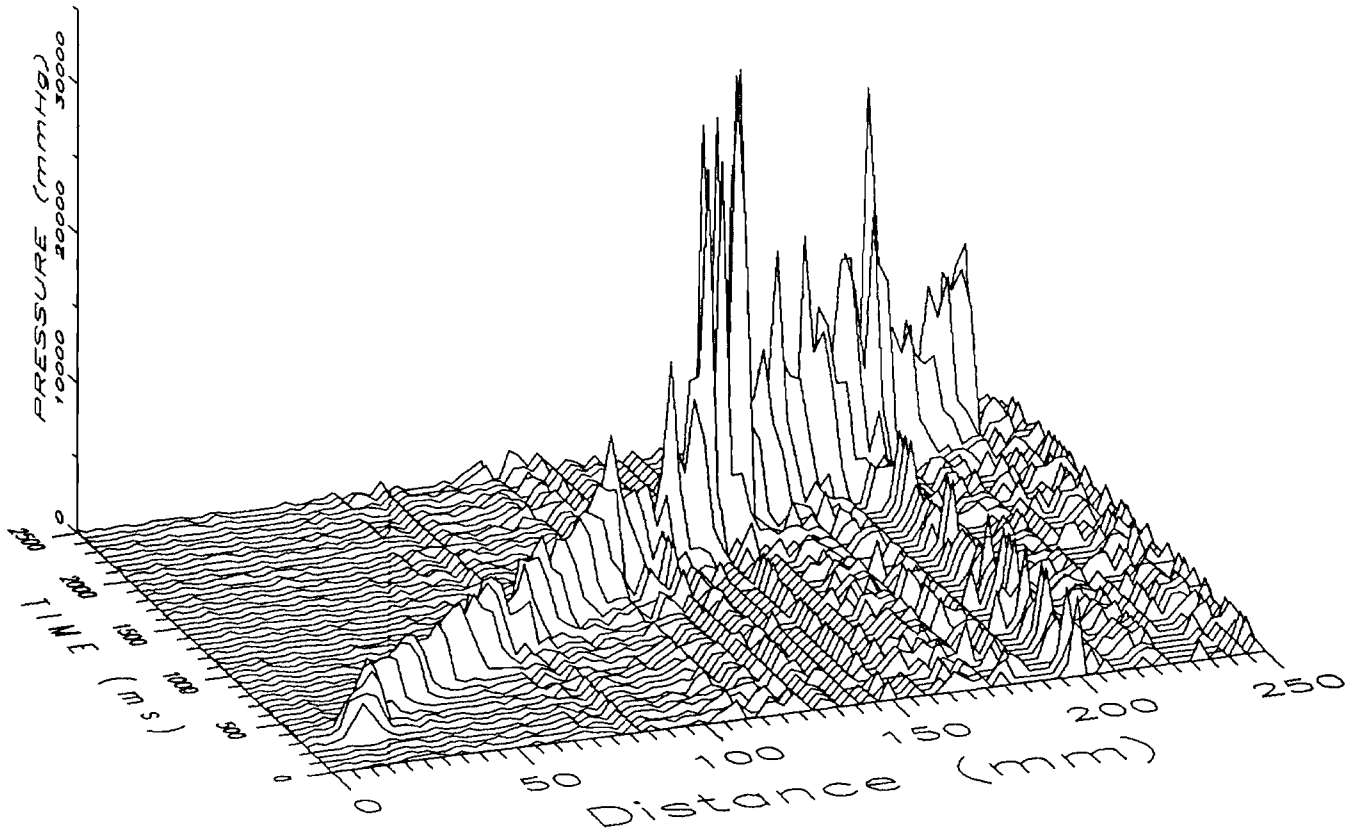

FIGURE 30: Pressure surface plot associated with a synthetic "normal" peristaltic contraction. The pressure ridge is readily discernable from the noisy background, though the uniformity of contraction rate or absolute pressure magnitudes are difficult to gage quantitatively.

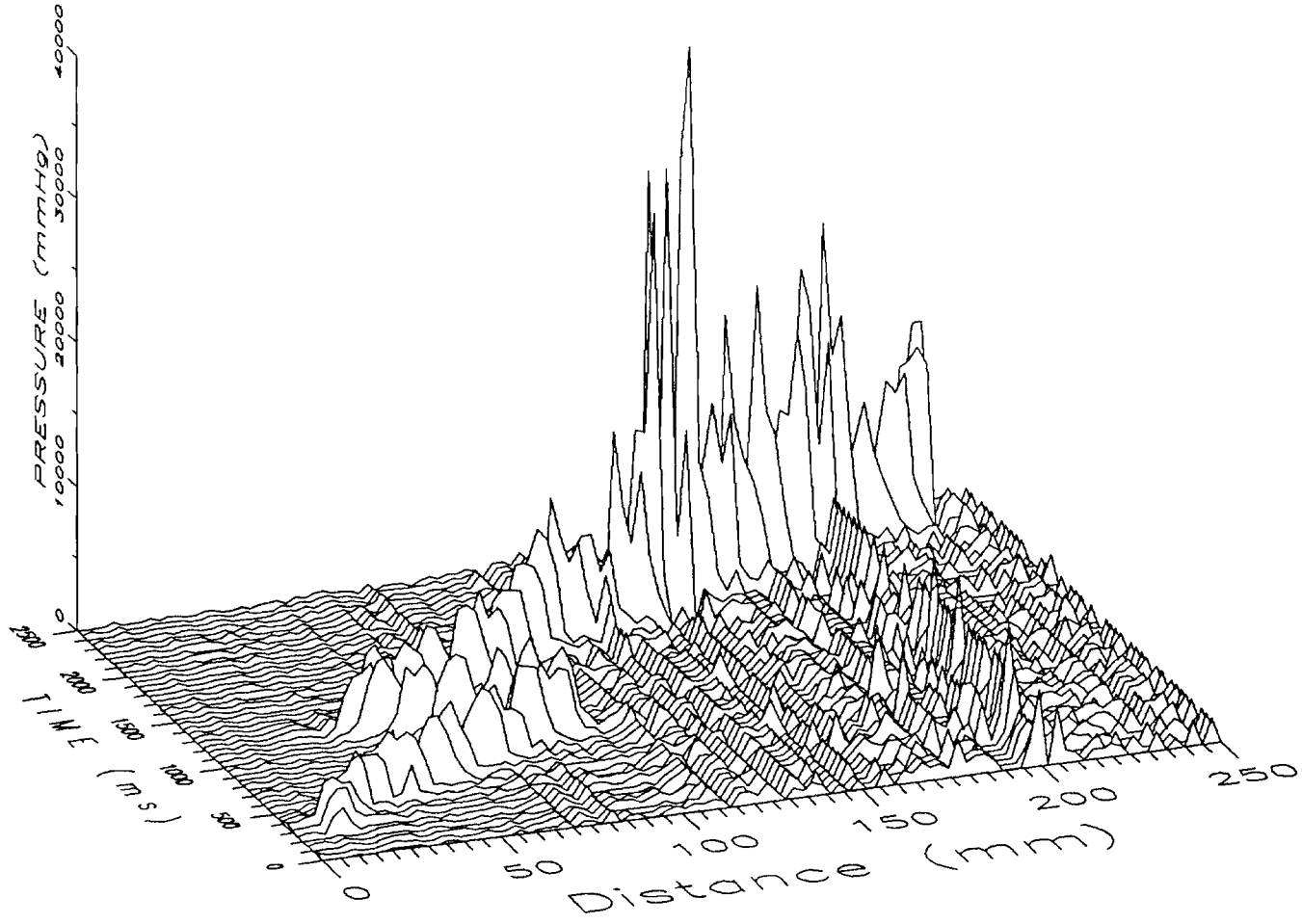

FIGURE 31: Pressure surface plot of a synthesized retrograde peristaltic contraction. Though an anomaly is visible, the exact nature is difficult to ascertain from this presentation of the data.

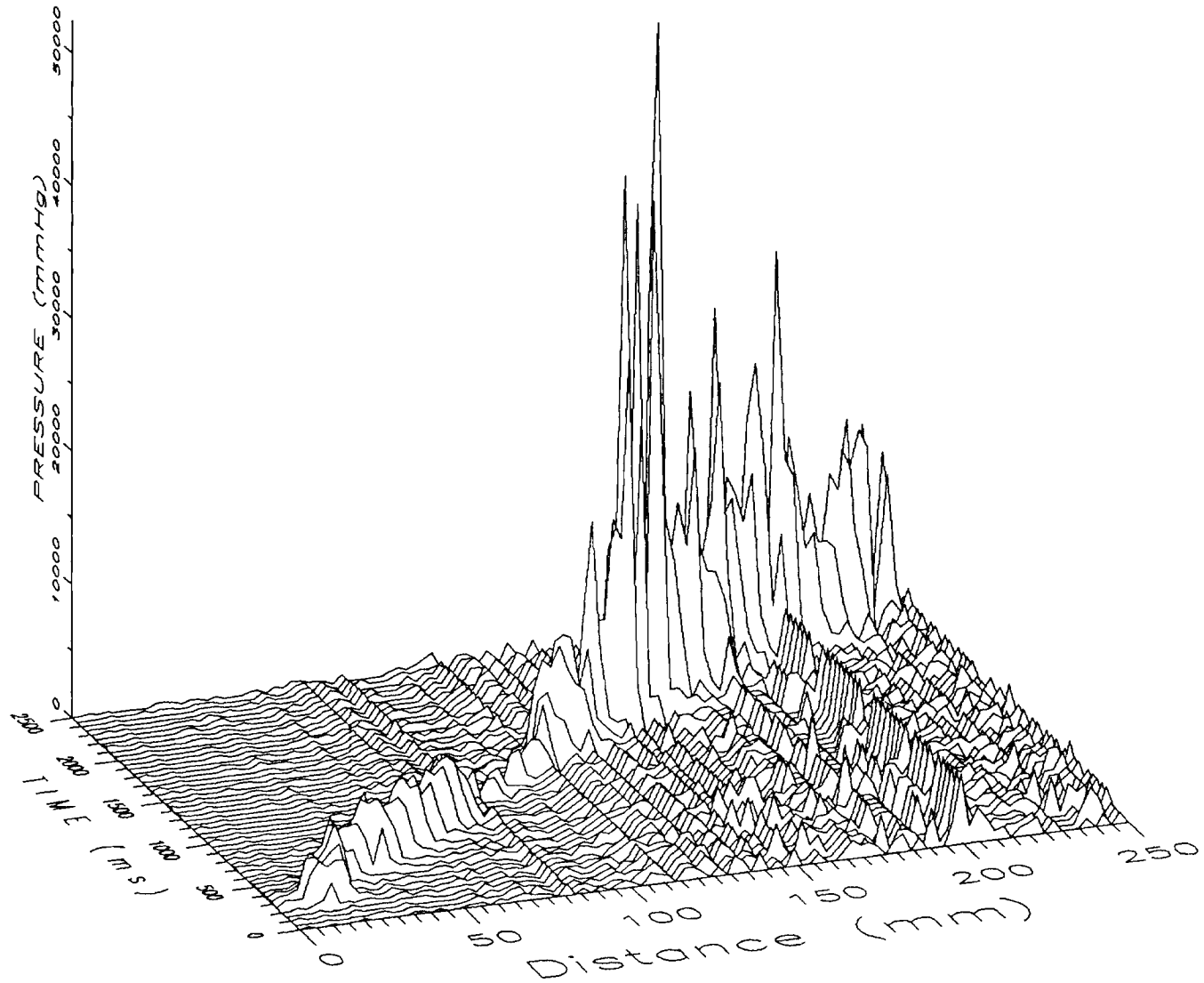

FIGURE 32: Pressure plot of a synthesized "weak" peristaltic contraction illustrating a dip in the pressure ridge around the 80 mm mark.

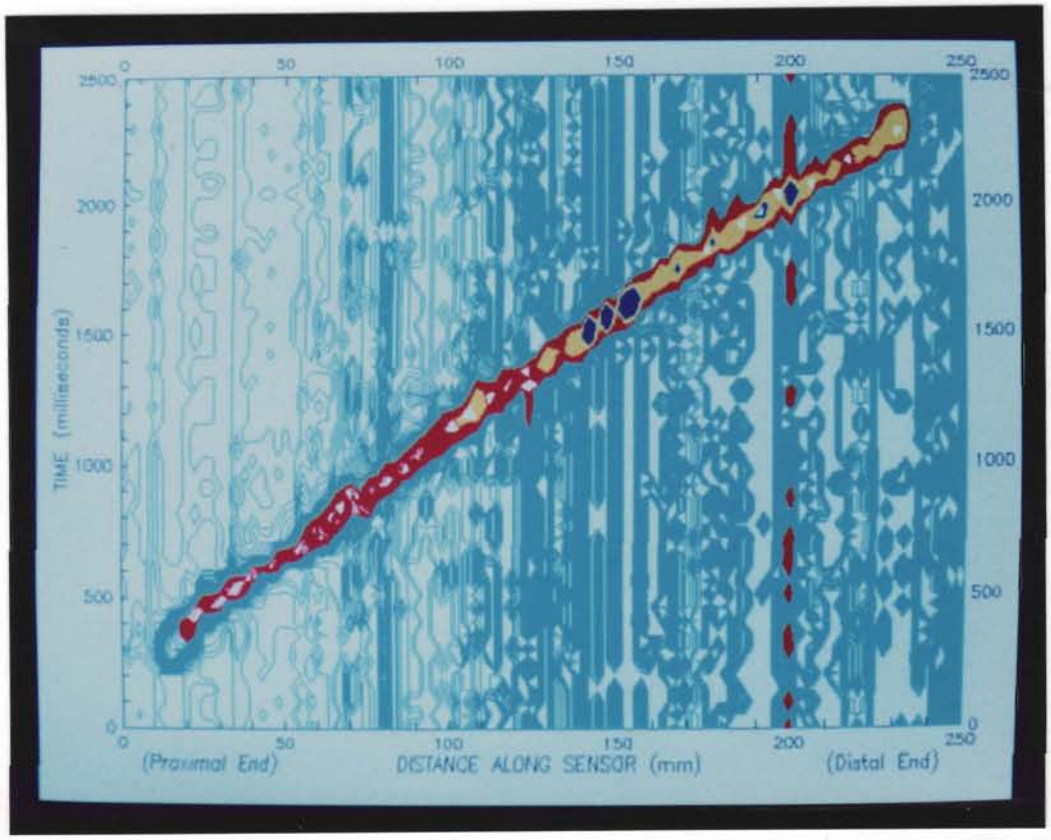

FIGURE 33: Colorized topographical plot of a synthetic "normal" peristaltic contraction (same data as Figure 30). The pressure ridge is readily discernable from the noisy background. Note the increasing intrusion of noise as the distance from the illumination injection point increases.

Pressure contours:

Green:	0	to	2000	mmHg
Red:	2000	to	5000	mmHg
Yellow:	5000	to	10000	mmHg
Blue:	10000+			mmHg

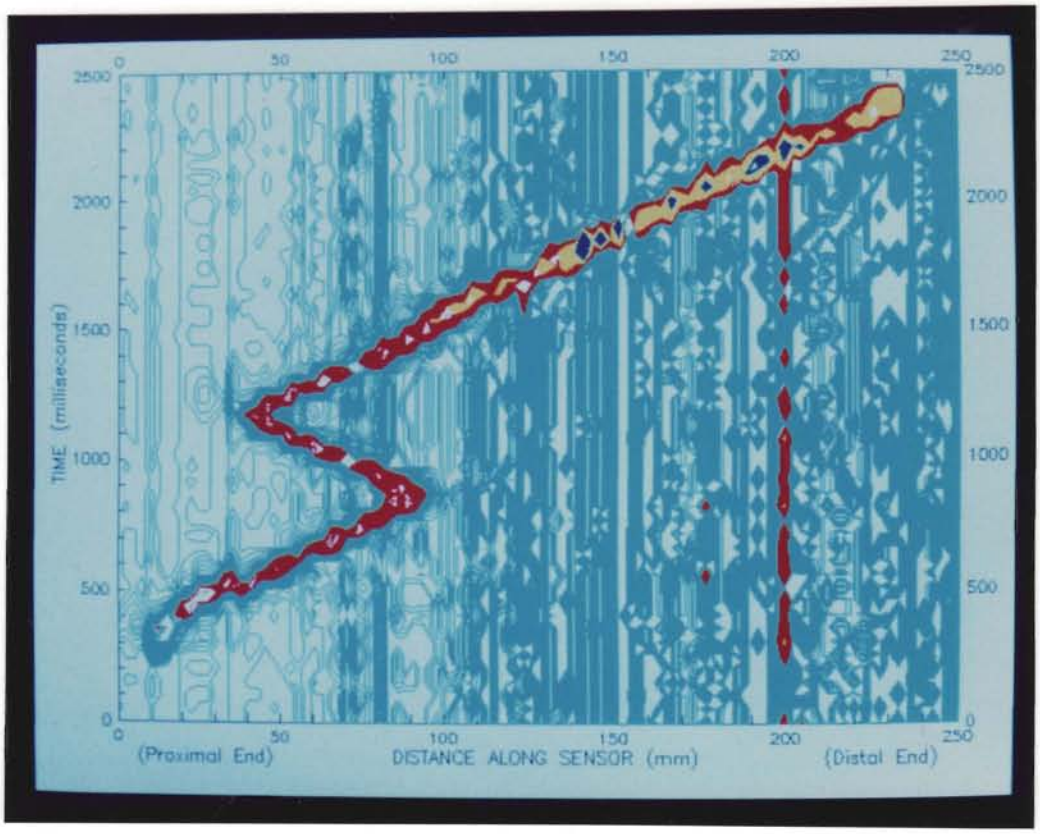

FIGURE 34: Colorized topographical plot of a synthesized retrograde peristaltic contraction (same data as Figure 31).

Pressure contours:

Green:	0	to	2000	mmHg
Red:	2000	to	5000	mmHg
Yellow:	5000	to	10000	mmHg
Blue:	10000+			mmHg

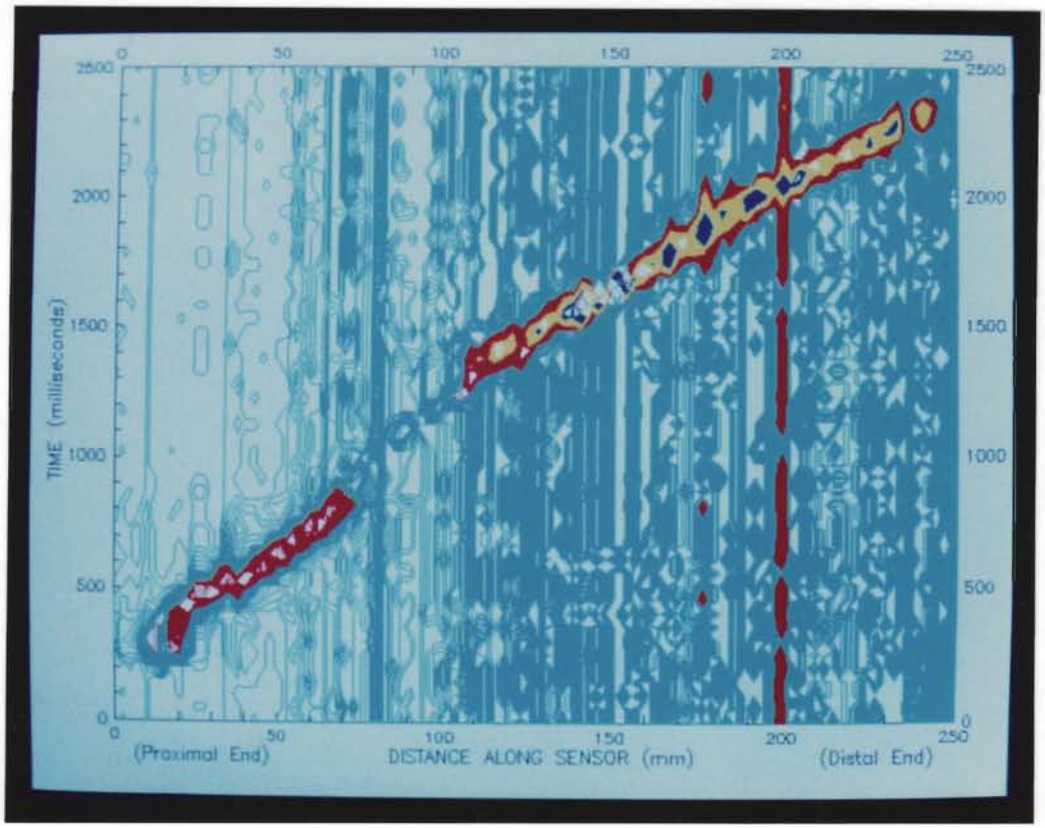

FIGURE 35: Colorized topographical plot of a synthesized "weak" peristaltic contraction (same data as Figure 32), clearly illustrating the pressure dip around the 80 mm mark.

Pressure contours:

Green:	0	to	2000	mmHg
Red:	2000	to	5000	mmHg
Yellow:	5000	to	10000	mmHg
Blue:	10000+			mmHg

As illustrated in Figure 29, the sphincter pressure sensor is attached to the distal end of the sensor probe. It consisted of 88 pressure sensor sites distributed over a cylindrical surface, with 8 sites uniformly spaced about the circumference in each of eleven layers. This resulted in a nearly uniform sensor spacing of 2.5 mm in the longitudinal and circumferential directions.

Tests on the cylindrical sensor were performed by subjecting it to pressures exerted by a synthetic rubber sphincter consisting of a soft rubber donut measuring 35 mm OD, 9 mm ID, and 14 mm thick. It was found that both uniform and nonuniform pressure distributions could be imparted to the cylindrical sensor by squeezing the periphery of the sphincter in the hand.

Satisfactory display of data from the cylindrical sensor proved to be more difficult than display of esophageal data because of the need to display information in four dimensions: pressure, time, axial sensor location, and circumferential sensor location. One data visualization approach considered was a "movie" display format in which time variant pressure, axial position, and circumferential position snapshots would be displayed adjacent to one another. The advantage of this approach was that data would be more intuitively presented as a series of pressure topographs as a function of time. However, with 50 scans per run to deal with, the approach to become too impractical due to the small size of each plot, the intensiveness of plotting, and the subsequent need by the user to integrate information dispersed over a relatively large viewing area.

The approach that was eventually selected was a variant of the above "movie" idea in which topographical plots of pressure versus time and circumferential position for the eleven different sensor layers were displayed in close proximity to one another. Thus, in contrast to one topographical plot for the esophageal pressure data, sphincter data would be presented in eleven adjacent topographical plots.

Figure 36, for example, shows the appearance of a normal sphincter contraction in which the pressure about the circumference is relatively uniform. In contrast, Figure 37 shows a contraction in which the pressure exerted by one quadrant was weaker than the others, and is graphically illustrated by the presence of a pressure dip at circumferential site number 4 of each sensor layer. However, despite the ability to present all pressure data in one plot, this approach is still not considered entirely satisfactory as the data is not presented in an intuitively useful manner, but is relatively abstract and requires more cognitive processing to interpret the data than the esophageal sensor plots shown earlier.

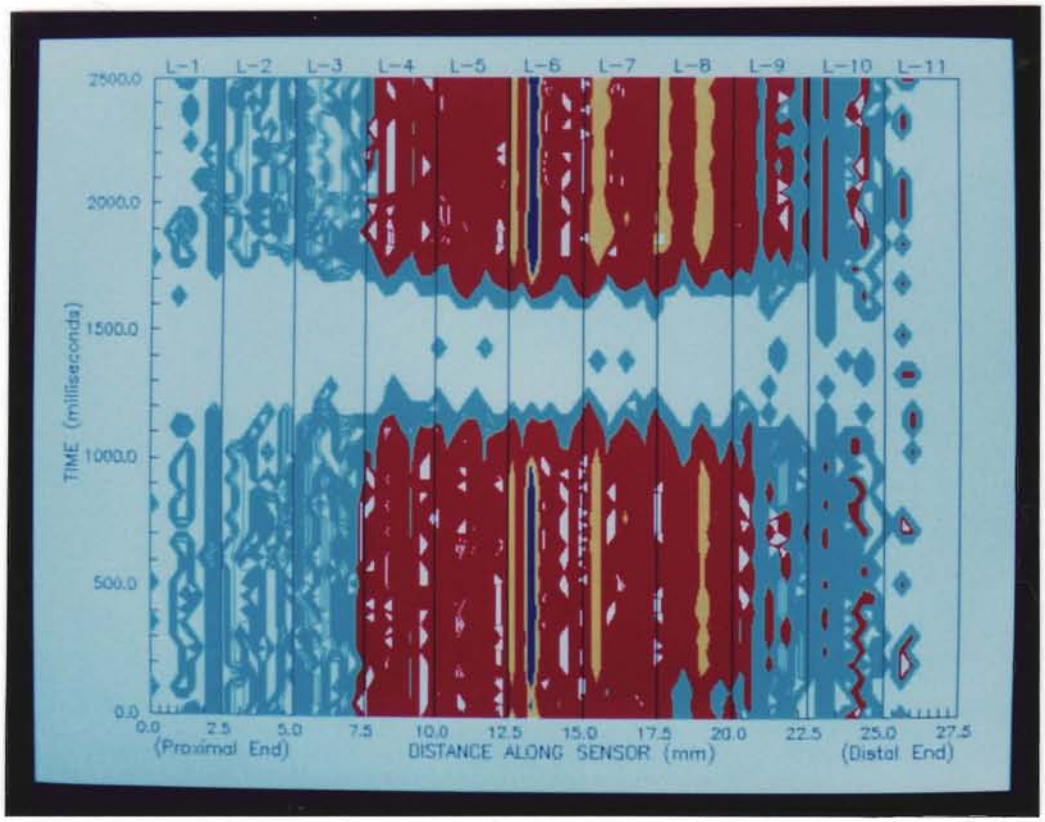

FIGURE 36: Uniform sphincter pressures measured by the cylindrical sensing region on the pressure sensor. Each vertical rectangle is a colorized topographical representation of the data within one of the eleven layers in the cylindrical sensor, and shows the pressure as a function of circumferential position (horizontal axis) and time (vertical axis).

Pressure contours:

Green:	0	to	1000	mmHg
Red:	1000	to	5000	mmHg
Yellow:	5000	to	7500	mmHg
Blue:	7500+			mmHg

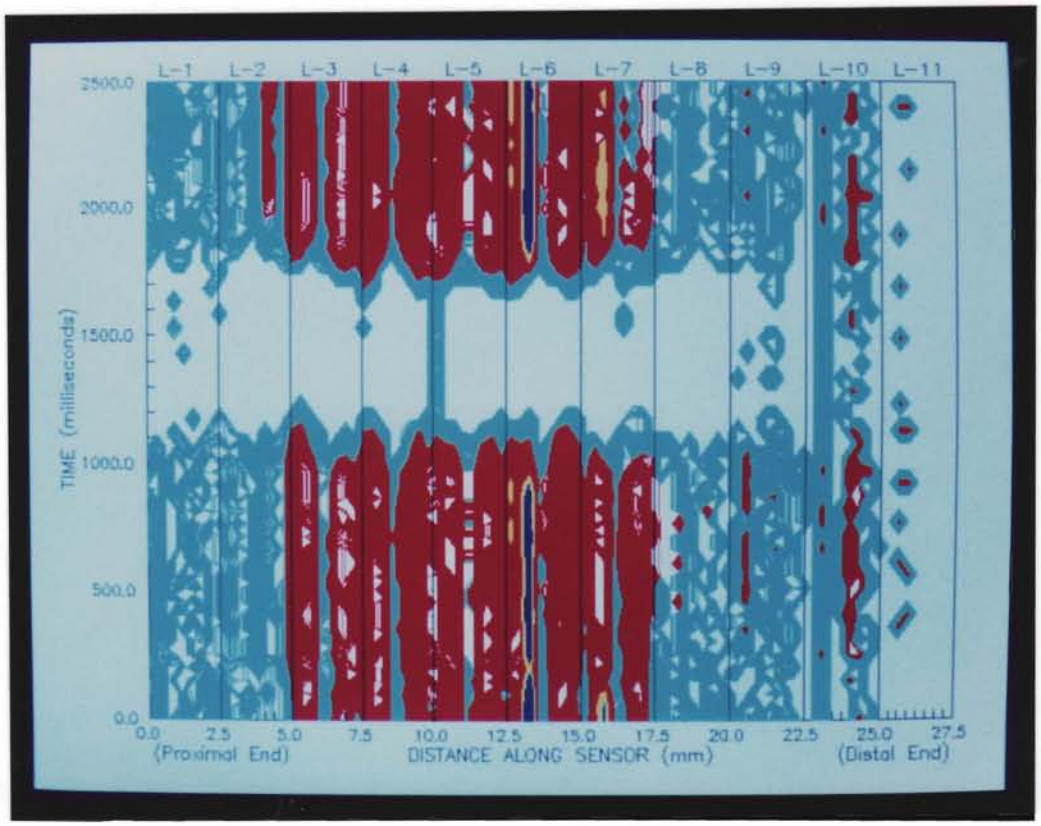

FIGURE 37: Colorized topographical representation of a weak contraction in one quadrant of the synthetic sphincter. The anomaly is revealed by the presence of low pressures in circumferential position number 4 of each layer in the cylindrical sensor.

Pressure contours:

Green:	0	to	1000	mmHg
Red:	1000	to	5000	mmHg
Yellow:	5000	to	7500	mmHg
Blue:	7500+			mmHg

2.4. Conclusions Regarding Technical Feasibility

Significant progress was made towards demonstrating the feasibility of developing a full-length flexible esophageal pressure sensor and monitor system. In this Phase I effort, it was shown that a fiberoptic, full-length sensor with 189 sensing sites could be fabricated, and that pressure data from synthetic esophageal peristaltic waves and sphincter contractions could be processed and displayed in a concise and intuitively-interpretable graphical format.

However, only a rigid sensor was designed and successfully fabricated, as a waveguide material that was simultaneously flexible and highly-transparent was not discovered. The rigid sensor was found to have a pressure sensitivity range of approximately 0 - 3,000 mmHg, and therefore not ideally suited to the measurement of esophageal and sphincter pressures which range from 0 - 200 mmHg.

On the whole, it is concluded that development of a full-length flexible esophageal monitor system is technically feasible, though significant additional work will need to be done in the future:

1. A continued search must be made for flexible waveguide materials with high transparency to reduce light losses along the length of the sensor. This issue might best be addressed by employing an expert consultant in the field of plastic materials, and also may require formulation of custom, non-commercial compounds.

2. Explore means of increasing the sensitivity of the sensor to those pressures encountered in the esophagus and sphincters. Again, an expert in plastic materials might be needed to specify a low-hysteresis, high-sensitivity transduction material.

3. Means should be explored of equalizing the light intensities emerging from the sensor fibers in the display array so as to more efficiently utilize the dynamic range of the CCD detector, e.g., placement of discrete customized filters over each sensor fiber or row of fibers in the display array.

4. Integrate and accelerate the functions of pressure data acquisition, calibration, processing, and display through the use of fast but inexpensive computers (e.g., 80386 machines). Additionally, explore alternative graphical data display modes to permit a more intuitive and concise method of displaying four-dimensional sphincter pressure data.

3. PROTOCOLS

The issue of protocols is not relevant to this program, as this research did not involve human or animal subjects.

4. PUBLICATIONS

In an effort to protect the proprietary and patent rights of the developments emerging from this grant, no publications have been made to date or contemplated for the near future.

5. INVENTIONS

Listed below are the titles of the invention reduced to practice during the period of this Phase I support, and fully described in this report:

"Esophageal and sphincter pressure monitor system utilizing a fiberoptic sensor."

6. REFERENCES

Begej, S., "An optical tactile sensor array," Proceedings of the SPIE Conf. Intelligent Robotics and Computer Vision, pp. 271-280, November, 1984.

Begej, S., A Tactile Sensing System and Optical Tactile Sensor Array for Robotic Applications, Technical Report 85-06, MS Thesis, Computer and Information Science Department, Univ. Massachusetts, Amherst, May, 1985.

Begej, S., Fingertip-Shaped Touch Sensor for Teleoperator and Robotic Applications, Final Report, Begej Corporation, Littleton, CO, NASA SBIR Phase I Contract No. NAS7-968, September, 1986.

Begej, S., "Fingertip-shaped optical tactile sensor for robotic applications," Proc. IEEE Int. Conf. Robotics and Automation, Philadelphia, PA, pp. 1752-1757, 25 April, 1988(a).

Begej, S., Tactile Telepresence System for Dexterous Telerobotics, Final Report, Begej Corporation, Littleton, CO, NASA SBIR Phase I Contract NAS7-1015, 29 August, 1988(b).

Begej, S., "Planar and fingertip-shaped tactile sensors for robotic applications," IEEE J. Robotics and Automation, vol. 4, no. 5, Oct, 1988(c).

7. LIST OF SUPPLIERS

Supplier	Product or Service
Devcon Corp. Danvers, MA 01923	Epoxy adhesives. S-33: 30 minute cure time. S-206: 5 minute cure time.
Dupont Co.	Acrylic optical fibers.
ESKA Co.	Acrylic optical fibers.
Golden Software, Inc. 809 14th Street PO Box 281 Golden, CO 80402	SURFER 3-D data plotting software, Version 4 (1990).
Norton Industrial Plastics PO Box 350 Akron OH 44309	Tygon polyurethane tubing
Polyoptics Corp.	Acrylic optical fiber
Scotch/3M Electrical Products Division St. Paul, MN, 55144	Self-fusing silicone tape, Number 70.

(File: c:\wp\report91\nih_psen.txt)